THE UNIVERSITY *of* EDINBURGH

Edinburgh Research Explorer

Quantifying uncertainty for predictions with model error in non-Gaussian systems with intermittency

OPEN ACCESS

Quantifying Uncertainty for Long Range Forecasting Scenarios with Model Errors in Non-Gaussian Systems with Intermittency.

Michal Branicki* and Andrew J. Majda

Department of Mathematics and Center for Atmosphere and Ocean Science,
Courant Institute of Mathematical Sciences, New York University, New York, USA,

Abstract

This article discusses a range of important mathematical issues arising in applications of a newly emerging stochastic-statistical framework for quantifying and mitigating uncertainties associated with prediction of partially observed and imperfectly modelled complex turbulent dynamical systems. The need for such a framework is particularly severe in climate science where the true climate system is vastly more complicated than any conceivable model; however, applications in other areas, such as neural networks and materials science, are just as important. The mathematical tools employed here rely on empirical information theory and fluctuation-dissipation theorems and it is shown that they seamlessly combine into a concise systematic framework for measuring and optimizing consistency and sensitivity of imperfect models. Here, we utilize a simple statistically exactly solvable 'perfect' system with intermittent hidden instabilities and with time-periodic features to address a number of important issues encountered in prediction of much more complex dynamical systems. These problems include the role and mitigation of model error due to coarse-graining, moment closure approximations, and the memory of initial conditions in producing short, medium and long range predictions. Importantly, based on a suite of increasingly complex imperfect models of the perfect test system, we show that the predictive skill of the imperfect models and their sensitivity to external perturbations is improved by ensuring their consistency on the statistical attractor (i.e., the climate) with the perfect system. Furthermore, the discussed link between climate fidelity and sensitivity via the fluctuation-dissipation theorem opens up an enticing prospect of developing techniques for improving imperfect model sensitivity based on specific tests carried out in the training phase of the unperturbed statistical equilibrium/climate.

1   Introduction

Contemporary climate change science is rapidly becoming a hotbed for the development of new mathematical ideas and techniques for dealing with the 'inevitable reality' when it comes to predicting the dynamical behavior of complex nonlinear systems given a limited knowledge of the system itself and partial observations. The Earth's climate is a perfect example of such an extremely complex and only partially known system coupling physical processes for the atmosphere, ocean, and land over a wide range of spatial and temporal scales (e.g., [11, 45]). The dynamical equations for the actual climate system are obviously unknown and all that is available are imperfect models and some coarse-grained observations of quantities like the mean or variance of temperature or greenhouse gases, or the large scale horizontal winds. Thus, a fundamental practical difficulty in estimating the sensitivity of the climate system lies in predicting the coarse-grained forced response of a nonlinear high-dimensional system from partial observations of the present unperturbed climate/attractor and imperfect models. The problem of mitigating the model error in imperfect predictions of complex nonlinear systems is an important and challenging one from both the practical and theoretical viewpoint. Many high-dimensional, nonlinear, multi-scale models display a

---

Corresponding author address: branicki@cims.nyu.edu

subtle but complex interplay between sensitivity to the perturbations and the nature of chosen parameterizations [22, 23, 44]. For example, contemporary cutting-edge projections of climate change are carried out through comprehensive coupled atmosphere-ocean simulation (AOS) models which necessarily parameterize some physical features such as clouds, sea ice cover, etc., as well as turbulent fluxes due to subgrid processes in the resolved dynamics [47, 45, 11, 51]. Consequently, the inevitable presence of intrinsic errors in these complex models makes the assessment of predictions for the coarse-grained, large-scale, long time trends a serious challenge. In turbulent systems this is compounded by the fact that energy often flows intermittently from the smaller unresolved scales to impact much larger and longer spatio-temporal scales of motion of interest [33]. Nevertheless, a systematic way of minimizing model error and improving the predictive performance of the imperfect models based the information obtained from the present climate remains a 'high priority target' driving developments in atmospheric/climate sciences, engineering, neural science, and applied mathematics.

Recently, a stochastic-statistical framework linking the unperturbed statistical attractor fidelity and sensitivity of imperfect models for capturing the true forced response in the 'climate change' scenario was proposed in [37, 38, 39, 17]. This newly emerging viewpoint blends detailed dynamical physical modeling and purely statistical analysis by combining empirical information theory with an appropriate fluctuation dissipation theorem and has at least two mathematically desirable features:

- The measure of skill in this approach is based on the relative entropy which, unlike other metrics predominantly based on RMS errors, is unbiased and invariant under the general change of variables [28, 27, 40, 41].

- The optimization principles based on the relative entropy 'metric' systematically minimize the lack of information in the imperfect model probability density relative to the perfect density. In contrast to independent tuning of the individual moments like the mean or covariance, this procedure minimizes the lack of information in the whole probability density over a subset of tunable parameters in the model.

Such an unambiguous and systematic procedure is particularly important when dealing with nonlinear high-dimensional models where responses of the statistical moments to parameter variations are nontrivially coupled. The use of relative entropy to improve imperfect models in a dynamic climate change context builds on earlier use of such concepts by statisticians for improving imperfect models [2, 6].

The goal of this paper is more modest in scope than developing practical implementations of this framework for use in comprehensive AOS or other high-dimensional models with a large number of both observables and physically constrained interdependent parameters. Before such attempts can be made, it is necessary to first understand various aspects of this approach in a hierarchy of controllable, simplified scenarios mimicking increasingly complex features of the vastly more complex true system. Here, we consider a simple, yet physically relevant and mathematically tractable, non-Gaussian test model with intermittently positive Lyapunov exponent due to transient instabilities in the resolved component; more realistic and complex analysis of this framework on a testbed combining the output an Atmospheric Global Cirulation Model (GCMs) and simplified spatially extended turbulent tracer models [36] are planned next. The single mode, non-Gaussian test model used here is given by a quadratically nonlinear system of coupled SDEs [46, 13] for a complex scalar with intermittent transient instabilities induced by stochastic fluctuations in the damping of the resolved component. Such transient instabilities are characteristic of turbulent nonlinear interactions between the resolved and unresolved scales and this work naturally complements the analysis initiated in [17] for Gaussian systems. This system has a surprisingly rich dynamics mimicking turbulent signals in various regimes of the turbulent spectrum (see figure 1), ranging from the energy transfer range with a very non-Gaussian dynamics with intermittency due to abundant short-lasting instabilities to a nearly-Gaussian laminar regime with essentially no instabilities. The imperfect models are obtained through various moment closure approximations and/or dimensional reduction. We show, using the tools of empirical information theory, that the imperfect models optimized for unperturbed

2

climate/attractor consistency also have a significantly improved skill for predicting the forced response in the 'climate change' scenario.

The important points discussed and illustrated throughout the paper for nonlinear, non-Gaussian systems with intermittency include the following:

- The information-theoretic optimization advocated here can dramatically improve predictive performance and forced response sensitivity of imperfect models to external perturbations (see also [37, 38, 39, 17]).

- Statistical attractor fidelity of imperfect models on the coarse-grained subset of resolved variables is necessary but not sufficient for high skill in predicting the true forced response to external perturbations in turbulent forced dissipative systems (see also [39]).

- There exist barriers to improvements within a given class of imperfect models beyond which the loss of information cannot be reduced except when this class is expanded to allow for more degrees of freedom (see [34, 17] for even simpler examples of information barriers).

- The information-theoretic optimization requires tuning the imperfect model marginal probability densities for the resolved variables to the densities of the perfect system on the unperturbed attractor. In the simplest Gaussian framework such a procedure implies simultaneous tuning of means and covariances [38, 39].

- The sensitivity of imperfect models for capturing the true forced response can be tested via algorithms exploiting a suitable fluctuation-dissipation theorem and experiments in the training phase in the unperturbed attractor/climate (see also [39, 17] and [22, 23] for implementations in atmospheric general circulation model (AGCM)).

- Nonlinear, non-Gaussian systems can have long memory of initial conditions, including the initial conditions for the unresolved processes, which might lead to significant errors in short and medium range predictions.

- Linear Gaussian imperfect models cannot reproduce the true nonlinear system response in the variance to forcing perturbations (see also [38, 39]).

The last fact pointed above is often overlooked in climate science literature (e.g., [50, 53, 48, 3, 49, 26]); consequences of these obvious shortcomings of the use of linear models for predicting forced response of nonlinear systems with positive Lyapunov exponents are illustrated in this paper in the simplest possible but revealing setting of non-Gaussian systems with hidden/unresolved intermittent instabilities. The first application of this stochastic-statistical framework was discussed in [17] for Gaussian systems which possessed a number of relevant features for geoscience and climate science applications such as seasonal cycle in both mean and covariance, a turbulent energy spectrum, and eddy diffusivity. This information-theoretical framework allowed for illustrating the impact of coarse-graining on quantifying model uncertainty at various spatial scales, the effects of over-dissipation of the imperfect turbulent velocity field, as well as the nontrivial dependence of the uncertainty in predictions for a turbulent tracer on the temporal structure of the zonal jet and the role of seasonality in making ensemble predictions. While the nomenclature of this paper is biased towards the climate science applications, there are many immediately obvious analogies throughout the text to problems involving high-dimensional nonlinear dynamical systems with non-trivial attractors in neural science, material science, or engineering.

The paper is organized as follows. In Section 2, we discuss the general principles of information theory in the context of improving climate/attractor fidelity of imperfect models (§22.1-2.2), as well as an important link [37, 38, 39] via the fluctuation-dissipation theory between the climate fidelity of imperfect models and their sensitivity to external perturbations (§22.3). In Section 3 we introduce the nonlinear and non-Gaussian 'perfect' test system with intermittently positive Lyapunov exponents which combines physically relevant features of turbulent systems with mathematical tractability. We then introduce a

suite of imperfect models associated with the non-Gaussian dynamics of the perfect system. Two of these imperfect models are nonlinear in the state variables but their statistics is 'Gausianized' through different moment closure approximations; the third imperfect model is linear and Gaussian. Next, in Section 4 we illustrate the utility of the stochastic-statistical framework in tough regimes with intermittency for optimization of the imperfect models and reduction of uncertainty in imperfect predictions. Conclusions and future research directions are presented in Section 5.

2 General principles of empirical information theory and fluctuation-dissipation theorems (FDT)

Applications of empirical information theory and the fluctuation-dissipation framework to climate change science have been addressed at length in [37, 38, 39, 17]. Therefore, below we only briefly summarize some concepts and notations for self-completeness of the present analysis. The fluctuation-dissipation framework is treated in more detail since it is crucial for the assessment of the forced response of the imperfect models based on information obtained from the unperturbed climate/statistical attractor, as discussed in the following sections.

2.1 Uncertainty quantification through empirical information theory

Consider for concreteness the Earth's climate system. While the actual equations governing climate dynamics on earth are unknown, it is natural to assume that these dynamics are Markovian, i.e., the future state depends only on the present state, on a suitably large space of variables $\boldsymbol{v} \in I\!\!R^P$, $P \gg 1$. Thus, it is reasonable to assume that the perfect dynamical system for the climate is given by

$$\dot{\boldsymbol{v}} = \boldsymbol{f}(\boldsymbol{v}, t) + \sigma(\boldsymbol{v})\dot{W}(t), \tag{1}$$

where σ is a $P \times K$ noise matrix with covariance Σ and $\dot{W} \in I\!\!R^K$ is K-dimensional white noise. The use of statistical descriptions for the climate system dates back to early predictability studies for simplified atmosphere models [30, 31, 32, 12].

The imperfect models are given by a known dynamical system

$$\dot{\boldsymbol{v}}_{\mathrm{M}} = \boldsymbol{f}^{\mathrm{M}}(\boldsymbol{v}_{\mathrm{M}}, t) + \sigma^{\mathrm{M}}(\boldsymbol{v}_{\mathrm{M}})\dot{W}_{\mathrm{M}}(t), \tag{2}$$

which has a similar structure to (1) but its phase space, $I\!\!R^M$, is typically completely different from that of the perfect system with $M \ll P$; the perfect system and its model share, however, the coarse-grained variables $\boldsymbol{u} \in I\!\!R^N$ where $N \leqslant P - M$. Throughout the following analysis we are interested in characterizing the statistical departures of the imperfect model dynamics relative to the perfect model on the subspace of the coarse-grained, resolved variables $\boldsymbol{u}$.

The evolution of the probability densities associated with the perfect and imperfect models satisfy appropriate Fokker-Planck equations which we omit here for brevity. The natural way [28, 41] to measure the lack of information in one probability density, say q, compared with the other, say p, is through the relative entropy, $\mathcal{P}(p, q)$, given by

$$\mathcal{P}(p, q) = \int p \ln \frac{p}{q}. \tag{3}$$

Despite the lack of symmetry in its arguments, the relative entropy, $\mathcal{P}(p, q)$ provides an attractive framework for assessing model error in AOS applications [27, 40, 7, 9, 1, 37, 5, 52, 20, 21, 38, 39] due to its two 'distance-like' properties: (i) $\mathcal{P}(p, q)$ is always positive unless $p = q$, and (ii) it is invariant under any invertible change of variables [40, 41]. Thus, in the context of uncertainty quantification, and especially in in AOS applications, the relative entropy (3) restricted to marginal densities on the common coarse-grained variables $\boldsymbol{u} \in I\!\!R^N$ provides the following useful diagnostic definitions:

- *Model error* is defined through the relative entropy as $\mathcal{P}(\pi, \pi^{\mathrm{M}})$ and it characterizes the lack of information in the marginal probability density of the imperfect model, π^{M}, relative to the true marginal density, π, on the coarse-grained variables $\boldsymbol{u}$ [37].

- *Internal prediction skill* of an imperfect model quantifies the role of initial conditions in the imperfect prediction of a future state of a system [27, 20, 21] and it represents the gain of information beyond the imperfect model climate (i.e., the probability density on the attractor). The internal prediction skill is expressed via the relative entropy as $\mathcal{P}(\pi^{\mathrm{M}}(\cdot|t_0), \pi_{att}^{\mathrm{M}})$ where $\pi^{\mathrm{M}}(\boldsymbol{u}, t|t_0)$ is the density with a given initial condition at time t_0 and $\pi_{att}^{\mathrm{M}}(\boldsymbol{u}, t)$ is the climate for the imperfect system on the coarse-grained variables $\boldsymbol{u}$. For the perfect system the additional information in the conditional density $\pi(\cdot, t|t_0)$ relative to the perfect climate π_{att}, given by $\mathcal{P}(\pi(\cdot|t_0), \pi_{att})$, is simply called the prediction skill. Note that high internal prediction skill (of the imperfect model) is only meaningful if the corresponding model error is small.

- *Model sensitivity* [37] quantifies the gain of information in the probability density of a perfect/imperfect system in response to external perturbations from its climate (attractor); it is expressed via the relative entropy as $\mathcal{P}(\pi_\delta, \pi_{att})$ for the perfect system, or as $\mathcal{P}(\pi_\delta^{\mathrm{M}}, \pi_{att}^{\mathrm{M}})$, where π_δ, π_δ^{M} are, respectively, the perturbed perfect and imperfect densities and π_{attr}, π_{att}^{M} are the corresponding marginal densities for the unperturbed (perfect and model) climate.

2.2   Improving climate fidelity of imperfect models

The framework of empirical information theory provides a convenient and unambiguous way of improving the performance of imperfect models both in terms of minimizing their error and increasing their sensitivity to external perturbations; the main facts are outlined below (see [38, 39] for additional details).

Consider first a class of imperfect models, $\mathcal{M}$; the best imperfect model on the coarse-grained variables $\boldsymbol{u}$ is characterized by the marginal density $\pi^{\mathrm{M}*}$, $\mathrm{M}_* \in \mathcal{M}$, so that the perfect model with the marginal density π has the smallest additional information beyond the imperfect model density [37], i.e.,

$$\mathcal{P}(\pi, \pi^{\mathrm{M}*}) = \min_{\mathrm{M} \in \mathcal{M}} \mathcal{P}(\pi, \pi^{\mathrm{M}}). \tag{4}$$

An important issue to contend with in any realistic scenario is the fact that the perfect model density, π, in (4) is not known and only its best unbiased estimate, π_L, based on L measurements $\bar{\boldsymbol{E}}_L$ of the perfect system during the training phase is available. The following general principle [35, 37] facilitates the practical calculation of (4)

$$\mathcal{P}(\pi, \pi_{L'}^{\mathrm{M}}) = \mathcal{P}(\pi, \pi_L) + \mathcal{P}(\pi_L, \pi_{L'}^{\mathrm{M}}), \tag{5}$$

where $L' \leq L$. Note that $\mathcal{P}(\pi_L, \pi_{L'}^{\mathrm{M}})$ exactly gives the lack of information in a 'coarse-grained' probability density associated with fewer constraints, $\pi_{L'}^{\mathrm{M}}$; this is an example of an information barrier which cannot be overcome unless more measurements are incorporated. Consequently, the optimization principle (4) can be computed by replacing the unknown π by the hypothetically known π_L so that the optimal model satisfies

$$\mathcal{P}(\pi_L, \pi_{L'}^{\mathrm{M}*}) = \min_{\mathrm{M} \in \mathcal{M}} \mathcal{P}(\pi_L, \pi_{L'}^{\mathrm{M}}), \qquad L' \leqslant L. \tag{6}$$

Climate fidelity [37, 38, 10], or statistical equilibrium fidelity, of an imperfect model consistent with the L measurements of the coarse-grained variables $\boldsymbol{u}$ arises when

$$\mathcal{P}(\pi_L, \pi_{L'}^{\mathrm{M}*}) = 0. \tag{7}$$

For simplicity in notation, and due to the form of (4) and (6), we skip the subscripts L and L' in the following discussion; the remaining assumption is that the number of the coarse-grained measurements of the imperfect model does not exceed the number of analogous measurements of the perfect system (i.e.,

$L' \leqslant L$). It turns out, as shown in the following sections, that even when the time-averaged climate fidelity is achieved, i.e.,

$$\overline{\mathcal{P}(\pi, \pi^{\mathrm{M}})} \equiv \int_0^T \mathcal{P}(\pi, \pi^{\mathrm{M}}) \ll 1, \tag{8}$$

with T the period on the attractor of the perfect system, a significant improvement in the model prediction skill and sensitivity can be achieved.

The most practical setup for utilizing the framework of empirical information theory in AOS applications arises when both the measurements of the perfect system and its imperfect model involve only the mean and covariance of the resolved variables $\boldsymbol{u}$ so that π_L is Gaussian with climate mean $\bar{\boldsymbol{u}}$ and covariance R, whereas π^{M} is Gaussian with model mean $\bar{\boldsymbol{u}}^{\mathrm{M}}$ and covariance R^{M}. In this case, $\mathcal{P}(\pi_L, \pi^{\mathrm{M}})$ has an explicit formula [27, 41] which is extensively used throughout this study

$$\mathcal{P}(\pi_L, \pi^{\mathrm{M}}) = \left[\tfrac{1}{2} (\bar{\boldsymbol{u}} - \bar{\boldsymbol{u}}^{\mathrm{M}}) R_{\mathrm{M}}^{-1} (\bar{\boldsymbol{u}} - \bar{\boldsymbol{u}}^{\mathrm{M}}) \right]$$

$$+ \tfrac{1}{2} \left[\mathrm{tr}[R R_{\mathrm{M}}^{-1}] - N - \ln \det[R\, R_{\mathrm{M}}^{-1}] \right]. \tag{9}$$

The first term in brackets in (9) is the signal, reflecting the model error in the mean but weighted by the inverse of the model variance, R_{M}, whereas the second term in brackets, the dispersion, involves only the model error covariance ratio, $R\, R_{\mathrm{M}}^{-1}$. The signal and dispersion terms in (9) are individually invariant under any (linear) change of variables which maps Gaussian distributions to Gaussians; this property is very important for unbiased model calibration.

2.3 The link between climate fidelity and sensitivity of imperfect models

We briefly outline here the framework developed in [38, 39] which directly links the uncertainty in the imperfect model projections for the forced response with the imperfect model fidelity to the unperturbed statistical equilibrium/climate.

Assume that the perfect system or the imperfect model or both are perturbed so that $\pi_\delta(\boldsymbol{u}, t)$ the unknown perfect distribution, $\pi_{L,\delta}(\boldsymbol{u}, t)$, its least-biased density based on L measurements, and $\pi_\delta^{\mathrm{M}}(\boldsymbol{u}, t)$ the model distribution all vary smoothly with the parameter δ, i.e.,

$$\pi_{L,\delta}(\boldsymbol{u}) = \pi_L(\boldsymbol{u}) + \delta\pi_L(\boldsymbol{u}), \qquad \int_{\mathbb{R}^N} \delta\pi_L(\boldsymbol{u})\mathrm{d}\boldsymbol{u} = 0,$$

$$\pi_\delta^{\mathrm{M}}(\boldsymbol{u}) = \pi^{\mathrm{M}}(\boldsymbol{u}) + \delta\pi^{\mathrm{M}}(\boldsymbol{u}), \qquad \int_{\mathbb{R}^N} \delta\pi^{\mathrm{M}}(\boldsymbol{u})\mathrm{d}\boldsymbol{u} = 0, \tag{10}$$

where we skipped the explicit time dependence of the densities. For stochastic dynamical systems rigorous theorems guarantee this smooth dependence under minimal hypothesis [24]. A simple instructive example corresponds to the Gaussian framework based on the measurements of the means and covariances only with $\pi_{L,\delta} = \pi_{G,\delta} \equiv \mathcal{N}(\bar{\boldsymbol{u}}, R)$, and $\pi_\delta^{\mathrm{M}} = \pi_{G,\delta}^{\mathrm{M}} \equiv \mathcal{N}(\bar{\boldsymbol{u}}^{\mathrm{M}}, R^{\mathrm{M}})$. Assuming further perfect fidelity in the unperturbed climate, $\mathcal{P}(\pi_G, \pi_G^{\mathrm{M}}) = 0$, and diagonal covariance matrices R and R^{M}, the leading order Taylor expansion in the (small) parameter δ of the error in the perturbed model density $\pi_{G,\delta}^{\mathrm{M}}$ relative to the true perturbed density $\pi_{G,\delta}$ leads to

$$\mathcal{P}(\pi_{G,\delta}, \pi_{G,\delta}^{\mathrm{M}}) = \mathcal{S}(\pi_{G,\delta}) - \mathcal{S}(\pi_\delta)$$

$$+ \frac{1}{2} \sum_{|k| \leq N} (\delta\bar{u}_k - \delta\bar{u}_k^{\mathrm{M}})\, R_k^{-1} \,(\delta\bar{u}_k - \delta\bar{u}_k^{\mathrm{M}})$$

$$+ \frac{1}{4} \sum_{|k| \leq N} R_k^{-2} \,(\delta R_k - \delta R_k^{\mathrm{M}})^2 + O(\delta^3). \tag{11}$$

6

(For a more general result for arbitrary densities see [38, 17].) The entropy difference, $\mathcal{S}(\pi_{\delta,G}) - \mathcal{S}(\pi_\delta)$, in (11) corresponds to the intrinsic error due to measuring only the mean and covariance of the perfect system while the remaining terms characterize the uncertainty due to the external perturbation; the first (second) summation in (11) is the signal (dispersion) contribution to the model error.

Given a class of imperfect models $\mathcal{M}$, the error (11) in predicting the true system's response to external perturbations is minimized for the model which is the most consistent with the unperturbed climate, i.e., the model $\text{M}_* \in \mathcal{M}$ satisfying (4) or (6). In fact, climate consistency of an imperfect model is a necessary but not a sufficient condition for its predictive skill, as shown in [38], where simple yet instructive examples reveal the possibility of intrinsic barriers to improving model sensitivity even with perfect climate fidelity. The only way to overcome such barriers is by extending the class of imperfect models to account for more degrees of freedom. In the following sections, we will present further examples of such situations in more complex non-Gaussian models.

2.3.1 FDT as a link between fidelity and sensitivity

The attractive feature of the fluctuation-dissipation framework for forced dissipative systems is that it allows one to estimate the expected response of the system to external perturbations by collecting lag-covariance statistics of the unperturbed attractor/climate. Below we list the most important features of this framework (see [35, 42, 16] for details) which will be necessary for the subsequent analysis of the sensitivity of the imperfect model sensitivity discussed in §4.3.3. For applications of the fluctuation dissipation theorem to estimate the linear response of the system defined by an atmospheric general circulation model (AGCM) see [22, 23].

Consider the time-periodic probability density such that $p_{att}(\boldsymbol{v}, s) = p_{att}(\boldsymbol{v}, s + T_0)$ on the attractor of the perfect system (1) satisfying the Fokker-Planck equation

$$\frac{\partial p_{att}}{\partial s} + \nabla_{\boldsymbol{v}}[p_{att}\,\boldsymbol{f}(\boldsymbol{v}, s)] - \frac{1}{2}\nabla_{\boldsymbol{v}} \cdot \nabla_{\boldsymbol{v}}[\sigma\sigma^T p_{att}] = 0. \tag{12}$$

Existence of such a statistical attractor with time-periodic density p_{att} can be established in systems which are dissipative in an appropriate sense [42]. Consequently, the statistics of some functional $A(\boldsymbol{v})$ on the attractor are determined by

$$\tilde{\langle A \rangle} = \frac{1}{T_0} \int_0^{T_0} \int_{I\!\!R^p} A(\boldsymbol{v}, s) p_{att}(\boldsymbol{v}, s) \mathrm{d}\boldsymbol{v} \mathrm{d}s. \tag{13}$$

Note that in such a framework p_{att} becomes an invariant probability measure on $I\!\!R^p \times S^1$ with

$$\frac{1}{T_0} \int_0^{T_0} \int_{I\!\!R^p} p_{att}(\boldsymbol{v}, s) \mathrm{d}\boldsymbol{v} \mathrm{d}s = 1. \tag{14}$$

Next, perturb both the perfect model (1) and the imperfect model (2) by $\delta \boldsymbol{w}(\boldsymbol{v}, s) f(t)$ to generate the perfect probability density, $p_\delta(\boldsymbol{v}, t)$, and the imperfect probability density, $p_\delta^{\text{M}}(\boldsymbol{v}^M, t)$ with the marginal densities on the common coarse-grained variables $\boldsymbol{u}$ given by

$$\begin{aligned}
\pi^{\text{M}}(\boldsymbol{u}, s, t) &= \pi_{att}^{\text{M}}(\boldsymbol{u}, s) + \delta\pi^{\text{M}}(\boldsymbol{u}, s, t), \\
\pi(\boldsymbol{u}, s, t) &= p_{att}(\boldsymbol{u}, s) + \delta\pi(\boldsymbol{u}, s, t).
\end{aligned} \tag{15}$$

Then, the time-periodic FDT [42] states that if the perturbation is small enough (and under some minimal hypothesis of smoothness of the unperturbed measure), the leading order correction to the statistics in (13) becomes

$$\delta\,\tilde{\langle A \rangle}\,(t) = \int_0^t R_A(t - s)\delta f(s)\mathrm{d}s, \tag{16}$$

where $R(t)$ is the linear response operator computed via the correlations in the unperturbed climate as

$$R(t) = \widetilde{\langle A(\boldsymbol{v}(t+s), t+s) \otimes B(\boldsymbol{v}(s), s) \rangle}. \tag{17}$$

with $\boldsymbol{v}(t+s)$ the solution of (1) with $\boldsymbol{v}|_{t_0} = u(s)$. The functional B in (17) is given by

$$B(\boldsymbol{v}, s) = -\frac{\mathrm{div}_{\boldsymbol{v}}(\boldsymbol{w}(\boldsymbol{v}, s)p_{att}(\boldsymbol{v}, s))}{p_{att}(\boldsymbol{v}, s)}. \tag{18}$$

We are interested in the best imperfect models which minimize $\mathcal{P}(\pi_\delta(t), \pi_\delta^{\mathrm{M}}(t))$ for a given prediction horizon t and perturbed forcing scenario, $\delta\boldsymbol{w}(\boldsymbol{v}, s)f(t)$. Assuming a smooth dependence of the perturbed densities on the parameter δ (as in (10)), the corresponding perturbed values of the coarse-grained functionals $\bar{\boldsymbol{E}}_{\delta, L}(t)$ and $\bar{\boldsymbol{E}}_{\delta, L}^{\mathrm{M}}(t)$ are defined through (13) and (15) by

$$
\begin{aligned}
\text{a)} \quad & \bar{\boldsymbol{E}}_{L,\delta}(t) = \int \boldsymbol{E}_L(\boldsymbol{u})\pi + \int \boldsymbol{E}_L(\boldsymbol{u})\delta\pi(t), \\
\text{b)} \quad & \bar{\boldsymbol{E}}_{L,\delta}^{\mathrm{M}}(t) = \int \boldsymbol{E}_L(\boldsymbol{u})\pi^{\mathrm{M}} + \int \boldsymbol{E}_L(\boldsymbol{u})\delta\pi^{\mathrm{M}}(t).
\end{aligned}
\tag{19}
$$

A potentially practical quantitative link between climate fidelity and prediction skill is defined through the fluctuation dissipation formulas in (16)-(18). First, by assuming the validity of FDT and a sufficiently small perturbation strength, $\delta f(t)$, one obtains

$$\int \boldsymbol{E}_L(\boldsymbol{u})\delta\pi(t) = \int_0^t R_{\boldsymbol{E}}(t-s)\delta f(s)ds + O(\delta^2), \tag{20}$$

where $R_{\boldsymbol{E}}$ is the corresponding linear response operator for the perfect system defined in (17); analogous formula holds for the imperfect system with $R_{\boldsymbol{E}}^{\mathrm{M}}$ and $\delta\pi^{\mathrm{M}}$. Now, with statistical equilibrium fidelity from (7) satisfied by the imperfect model the leading term in (19a) equals the leading order term in (19b) so that $\mathcal{P}(\pi_{L,\delta}, \pi_\delta^{\mathrm{M}})$ vanishes identically at $\delta = 0$ and the perturbation formulas in (11) and (17) can be applied directly with the approximation in (20) from FDT. For example, if u is a scalar variable like the global temperature with the two measurements $\bar{\boldsymbol{E}} = (\bar{u}, \sigma^2)$ of the mean $\bar{u}$ and the variance σ^2, then combining (11) with the FDT formulas (15) and (20) yields

$$
\begin{aligned}
\mathcal{P}(\pi_\delta(t), \pi_\delta^{\mathrm{M}}(t)) &= \mathcal{S}(\pi_{G,\delta}(t)) - \mathcal{S}(\pi_\delta(t)), \\
&+ \frac{1}{2}\sigma^{-2}\left(\int_0^t \left(R_{\bar{u}}(t-s) - R_{\bar{u}}^{\mathrm{M}}(t-s)\right)\delta f(s)ds\right)^2 \\
&+ \frac{1}{4}\sigma^{-4}\left(\int_0^t \left(R_{\bar{\sigma}^2}(t-s) - R_{\bar{\sigma}^2}^{\mathrm{M}}(t-s)\right)\delta f(s)ds\right)^2 + O(\delta^2).
\end{aligned}
\tag{21}
$$

In (21), σ^2 is the statistical equilibrium variance of both the perfect and imperfect models which coincide for perfect equilibrium fidelity and $R_{\bar{u}}$, $R_{\bar{u}}^{\mathrm{M}}$ and $R_{\bar{\sigma}^2}$, $R_{\bar{\sigma}^2}^{\mathrm{M}}$ are the mean and variance linear response operators. The formula in (21) and its generalizations to the multi-dimensional case illustrate that the skill of an imperfect model in predicting forced changes for the statistical equilibrium with general external forcing is directly linked to the skill in estimating the linear response operators for the mean and variance in a suitably weighted fashion as dictated by information theory.

2.3.2 Quasi-Gaussian FDT

In any realistic situation the exact density, p_{att}, on the unperturbed attractor of the perfect system is not known and some approximation is needed. The simplest approach relies on assuming a Gaussian density with the same mean and covariance as in the original system (e.g., [29, 35, 22, 23, 39]. In such a

quasi-Gaussian approximation (qG-FDT) the functional B in (18) is evaluated with $p_{att} = p_{att}^G$, while the lag-covariances in (17) are computed over the true non-Gaussian equilibrium measure from time averages assuming mixing and ergodicity. High skill of this approach was reported for estimating the linear response of a system defined by the atmospheric general circulation model (AGCM) in [22, 23].

2.3.3 Kicked FDT

The advantage of utilizing the FDT approximation is that the predictive skill of the imperfect model response operator $R_{\boldsymbol{E}}^{\mathrm{M}}(t)$ to external forcing can be evaluated through specific experiments in the training period where the fidelity with observed data of the perfect model can be monitored [39]. To see this, perturb the initial data for the perfect system and its imperfect model in the direction $\delta \boldsymbol{u}$ in a statistical fashion so that one generates statistical solutions, $p(\boldsymbol{v}, s, t)$ and $p^{\mathrm{M}}(\boldsymbol{v}, s, t)$, on $I\!\!R^P \times T^2$ and $I\!\!R^M \times T^2$ respectively with perturbed initial data,

$$\frac{\partial p^{\mathrm{M}}}{\partial t} = L_{FP}^M p^{\mathrm{M}}, \quad p^{\mathrm{M}}\Big|_{t=t_0} = p_{att}^{\mathrm{M}}(\boldsymbol{v}^{\mathrm{M}} - \delta \boldsymbol{u}, s),$$

$$\frac{\partial p}{\partial t} = L_{FP} p, \qquad p\Big|_{t=t_0} = p_{att}(\boldsymbol{v} - \delta \boldsymbol{u}, s). \tag{22}$$

It is a general mathematical fact [35, 39] that for δ small enough the linear response operators can be calculated from (22) as

$$\delta R_{\boldsymbol{E}}^{\mathrm{M}}(t) = \frac{1}{T_0} \int_0^{T_0} \int \boldsymbol{E}(\boldsymbol{u}) \delta \pi^{\mathrm{M}}(\boldsymbol{u}, s, t) \mathrm{d}\boldsymbol{u} \mathrm{d}s + O(\delta^2), \tag{23}$$

where $\delta \pi^{\mathrm{M}}$ is the perturbation of the marginal distribution in $\boldsymbol{u}$ of p^{M} given by (15); analogous result holds for the perfect model response operator $R_{\boldsymbol{E}}$. Thus, model errors in the training period for a given imperfect model can be assessed with the tools of information theory [37, 35, 41] such as (11) and (17) above by utilizing super-ensembles for the specific kicked ensemble perturbations for p^{M} given in (22); furthermore, in this training period, $R_{\boldsymbol{E}}(t)$ does not need to be calculated explicitly but only the statistical fidelity of $\int \int \boldsymbol{E}(\boldsymbol{u}) \delta p^{\mathrm{M}}(\boldsymbol{u}, s, t) \mathrm{d}\boldsymbol{u} \mathrm{d}s$ with the actual observed data in nature.

3 Complex scalar model with intermittently positive Lyapunov exponent

In order to illustrate the utility of the stochastic-statistical framework summarized above to non-Gaussian systems and their imperfect models, we first introduce a non-Gaussian exactly solvable model for a complex scalar with hidden transient instabilities and intermittency in the dynamics of the resolved component. Here, the resolved variable can be regarded as a single Fourier mode of a turbulent spatially extended system with the complex nonlinear interactions between various scales replaced by a stochastic drag and additive white noise forcing [43, 8]. This stochastic approach allows for analyzing many properties which are relevant for Uncertainty Quantification (UQ) and prediction in high-dimensional turbulent systems in a greatly simplified one-mode setting. Below we introduce three imperfect models which are obtained from the perfect system via various moment closure approximations and/or dimensional reduction; two of these models are nonlinear with 'Gaussianized' statistics while the simplest model is both linear and Gaussian. Analysis of model errors introduced by these different approximations and ways of mitigating these errors are discussed in §4.

3.1 The nonlinear model

Consider a single Fourier mode of a turbulent signal modeled by the following stochastic system (see [15, 14, 4])

$$(a) \quad \mathrm{d}u(t) = \big[(-\gamma(t)+i\omega)u(t)+b(t)+F(t)\big]\mathrm{d}t+\sigma_u \mathrm{d}W_u(t),$$

$$(b) \quad \mathrm{d}b(t) = \big[(-\gamma_b+i\omega_b)(b(t)-\hat{b})\big]\mathrm{d}t+\sigma_b \mathrm{d}W_b(t), \tag{24}$$

$$(c) \quad \mathrm{d}\gamma(t) = -d_\gamma(\gamma(t)-\hat{\gamma})\mathrm{d}t+\sigma_\gamma \mathrm{d}W_\gamma(t),$$

where W_u, W_b are independent complex Wiener processes and W_γ is a real Wiener process. There are nine parameters in the system (24): two damping parameters $\gamma_b, d_\gamma > 0$, two oscillation frequencies ω and ω_b, two stationary mean terms $\hat{b}$ and $\hat{\gamma}$ and noise amplitudes $\sigma_u, \sigma_b, \sigma_\gamma > 0$; F is a deterministic forcing which we assume to have the following special time-periodic form with a non-zero mean A_0 and given by

$$F(t) = A_0 + A_1 \cos(\omega t + \phi_1) + A_2 \cos(2\omega t + \phi_2), \tag{25}$$

where $\omega = \pi/6$ which ensures that the period $T_0 = 12$ so that it can be interpreted as a year consisting of 12 months; the forcing has two frequencies so that the equilibrium statistics of (24) has a more variable structure.

Here, we regard $u(t)$ as representing one of the resolved modes in a turbulent signal where the nonlinear mode-interaction terms are replaced by a stochastic drag $\gamma(t)$ and an additive noise term $b(t)$, as is often done in turbulence models [43, 8]. The nonlinear system (24), introduced first in [15] for filtering multiscale turbulent signals with hidden instabilities, has a number of attractive properties as a test model in our analysis. Firstly, it has a surprisingly rich dynamics mimicking turbulent signals in various regimes of the turbulent spectrum, including intermittently positive finite-time Lyapunov exponents, as discussed below [4]. Secondly, due to the particular structure of the nonlinearity in (24), exact path-wise solutions and exact second-order statistics of this non-Gaussian system can be obtained analytically, as discussed in [18, 19, 15]. The mathematical tractability of this model and its rich dynamical behavior provides a perfect test bed for analyzing effects of errors due to various moment closure approximations and dimensional reduction in a suite of imperfect models introduced in §3b.

3.1.1 Dynamical regimes of the perfect model

A number of dynamical regimes of the model (24) characterized by stability of the mean dynamics were determined in [4]. The physically relevant dynamical regimes of (24) satisfying the mean-stability condition

$$\chi = -\hat{\gamma} + \frac{\sigma_\gamma^2}{2d_\gamma^2} < 0, \tag{26}$$

with $\hat{\gamma}$ the mean damping in $u(t)$, and d_γ, σ_γ the damping and the noise variance in (24c), respectively, are (see also figure 1 for an illustration):

(I) *Regime of plentiful, short-lasting transient instabilities in the resolved component $u(t)$ with fat-tailed marginal equilibrium PDF.* This type of dynamics is characteristic of the turbulent energy transfer range and in the model (24); it occurs for $\sigma_\gamma, d_\gamma \gg 1$, $\sigma_\gamma/d_\gamma \sim \mathcal{O}(1)$ and $\hat{\gamma}$ sufficiently large so that $\chi < 0$. This is a regime of rapidly decorrelating damping fluctuations $\gamma(t)$ and the decorrelation time of $u(t)$ given approximately by $1/\hat{\gamma}$ (see [4]).

(II) *Regime of intermittent large-amplitude bursts of instability in $u(t)$ with fat-tailed marginal equilibrium PDF.* This regime is characteristic of turbulent modes in the dissipative range and it occurs for small σ_γ, d_γ, with $\sigma_\gamma/d_\gamma \sim \mathcal{O}(1)$ and $\hat{\gamma}$ sufficiently large so that $\chi < 0$.

Here, the decorrelation time of the damping fluctuations $\gamma(t)$ is long but the decorrelation time of fluctuations in $u(t)$ can vary widely, as in regime (I).
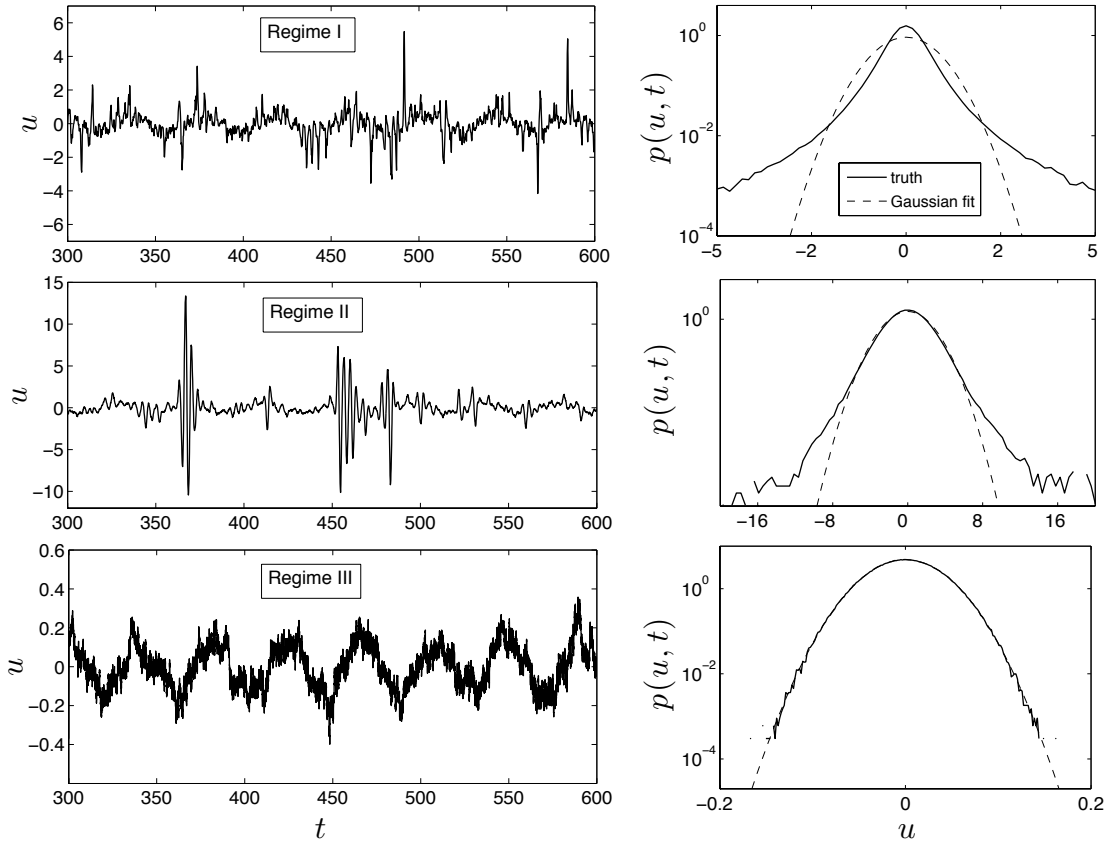
Figure 1: **Perfect system dynamics**. Schematic illustration of path-wise dynamics (left) and time-periodic statistics (at fixed time) on the attractor (right) in two intermittent regimes of system (24); the intermittent regimes are discussed in §3.1.1.

(III) *'Laminar' regime with nearly Gaussian equilibrium PDF.* This regime is characteristic of the laminar modes in the turbulent spectrum. Here, the transient instabilities in $u(t)$ occur very rarely. This type of dynamics occurs in (24) for $\hat{\gamma}^2 \gg \sigma_\gamma^2/2d_\gamma$ and $\chi < 0$.

3.2 The imperfect models

We describe here three imperfect models derived from (24) which introduce model errors through moment closure approximations or a dimensional reduction of the perfect system. We first note that, with the state vector $\boldsymbol{v} = (u, b, \gamma)^T$ with one resolved component u and two hidden components (b, γ), the deterministic part in (24) can be written as

$$\boldsymbol{f}(\boldsymbol{v}, t) = \hat{L}(t)\boldsymbol{v} + \mathbf{B}(\boldsymbol{v}, \boldsymbol{v}, t) + \mathbf{F}(t), \tag{27}$$

with $\hat{L}$ a linear operator, $\mathbf{B}$ a bilinear function, and $\mathbf{F}$ a spatially uniform term representing generalized deterministic forcing; the exact form of these terms can be easily obtained by comparing (27) with (24) and (1). In what follows we will skip the explicit dependence on time in $\boldsymbol{f}$ in order to simplify the notation.

It can be easily shown (e.g., [25, 4]) that by adopting an analogue of the averaged Reynolds decomposition of the state vector, $\boldsymbol{v} = \bar{\boldsymbol{v}} + \boldsymbol{v}'$, such that $\overline{\boldsymbol{v}'} = 0$ and $\overline{\bar{v}_i v'_j} = 0$, the evolution of the mean $\bar{\boldsymbol{v}}$ and

11

covariance $R \equiv \overline{\boldsymbol{v}' \boldsymbol{v}'^T}$ for the process $\boldsymbol{v}$ satisfying (1) is given by

$$a) \quad \dot{\bar{\boldsymbol{v}}} = \boldsymbol{f}(\bar{\boldsymbol{v}}) + \overline{\mathbf{B}(\boldsymbol{v}', \boldsymbol{v}')},$$

$$b) \quad \dot{R} = R\,A^T(\bar{\boldsymbol{v}}) + A(\bar{\boldsymbol{v}})R + \Sigma + \overline{\boldsymbol{v}'\mathbf{B}^T(\boldsymbol{v}', \boldsymbol{v}') + \mathbf{B}(\boldsymbol{v}', \boldsymbol{v}')\boldsymbol{v}'^T},$$

(28)

where A is the Jacobian of $\boldsymbol{f}$ at $\bar{\boldsymbol{v}}$, i.e., $A(\bar{\boldsymbol{v}}) \equiv \nabla \boldsymbol{f}(\bar{\boldsymbol{v}})$ and the overbar denotes an ensemble average.

Due to the particular form of the quadratic nonlinearity in the perfect system (24), exact formulas for the second-order statistics and path-wise solutions can be derived [15] without the explicit knowledge of the associated time-dependent probability density. Derivation of imperfect models in this framework utilizes some type of moment closure approximation of the terms

$$\overline{\mathbf{B}(\boldsymbol{v}', \boldsymbol{v}')} \quad \text{and} \quad \overline{\boldsymbol{v}'\,\mathbf{B}^T(\boldsymbol{v}', \boldsymbol{v}') + \mathbf{B}(\boldsymbol{v}', \boldsymbol{v}')\,\boldsymbol{v}'^T},$$

in (28) which involve the second and third moments of the fluctuations, respectively. Below we describe two nonlinear and one linear imperfect model of the system (24) which introduce model error due to various moment closure approximations applied to (28) and/or due to a dimensional reduction. The effects of errors introduced by these models on the short, medium and long range prediction skill, as well as ways of mitigating these errors via inflation of stochastic forcing, are discussed in the following sections. It is important to foreshadow the following discussion and stress that while all the imperfect models considered below have Gaussian statistics due to the moment closure approximations, the first two models remain nonlinear in the state variables $\boldsymbol{v} = (u, b, \gamma)$.

3.2.1 Gaussian Closure model (GCm)

The quasi-Gaussian closure approximation (e.g., [25]) results in a model which is nonlinear in the state variables and has Gausianized statistics; this simple closure familiar from turbulence theory implies neglecting the third and higher moments of the true probability density $p(\boldsymbol{v}, t)$ associated with the process $\boldsymbol{v}$ satisfying (24). For quadratic models and, in particular, for (24) only the third moments have to be neglected, i.e., GCm assumes

$$\overline{\boldsymbol{v}'_{\mathrm{M}}\,\mathbf{B}^T(\boldsymbol{v}'_{\mathrm{M}}, \boldsymbol{v}'_{\mathrm{M}}) + \mathbf{B}(\boldsymbol{v}'_{\mathrm{M}}, \boldsymbol{v}'_{\mathrm{M}})\,\boldsymbol{v}'_{\mathrm{M}}}^T = 0 \tag{29}$$

in (28b) with $\boldsymbol{v}_{\mathrm{M}} = (u_{\mathrm{M}}, b_{\mathrm{M}}, \gamma_{\mathrm{M}})$, $\boldsymbol{v}_{\mathrm{M}} = \bar{\boldsymbol{v}}_{\mathrm{M}} + \boldsymbol{v}'_{\mathrm{M}}$. The closure (29) results in a fully coupled dynamical system for the second-order statistics given by

$$a) \quad \dot{\bar{\boldsymbol{v}}}_{\mathrm{M}} = \boldsymbol{f}(\bar{\boldsymbol{v}}_{\mathrm{M}}) + \overline{\mathbf{B}(\boldsymbol{v}'_{\mathrm{M}}, \boldsymbol{v}'_{\mathrm{M}})},$$

$$b) \quad \dot{R}_{\mathrm{M}} = R_{\mathrm{M}}\,A^T(\bar{\boldsymbol{v}}_{\mathrm{M}}) + A(\bar{\boldsymbol{v}}_{\mathrm{M}})\,R_{\mathrm{M}} + \Sigma_{\mathrm{M}},$$

(30)

with $A(\bar{\boldsymbol{v}}_{\mathrm{M}}) = \nabla \boldsymbol{f}(\bar{\boldsymbol{v}}_{\mathrm{M}})$. Note that the system (30) represents the exact evolution of the second-order statistics for any Gaussian process where (29) is satisfied identically. Otherwise, the closure introduces a model error due to (29). Details on deriving GCm from the perfect system (24) are discussed in [4].

3.2.2 Deterministic-Mean model (DMm)

The mean and covariance in DMm evolve according to

$$a) \quad \dot{\bar{\boldsymbol{v}}}_{\mathrm{M}} = \boldsymbol{f}(\bar{\boldsymbol{v}}_{\mathrm{M}}),$$

$$b) \quad \dot{R}_{\mathrm{M}} = R_{\mathrm{M}}\,A^T(\bar{\boldsymbol{v}}_{\mathrm{M}}) + A(\bar{\boldsymbol{v}}_{\mathrm{M}})R_{\mathrm{M}} + \Sigma_{\mathrm{M}},$$

(31)

with $A(\bar{\boldsymbol{v}}_{\mathrm{M}}) \equiv \nabla \boldsymbol{f}(\bar{\boldsymbol{v}}_{\mathrm{M}})$ and initial conditions $\boldsymbol{v}_{\mathrm{M}}(t_0) = \boldsymbol{v}_0$, $R_{\mathrm{M}}(t_0) = R_0$. Similarly to GCm, DMm neglects the third and higher moments in the evolution of the covariance, R_{M}, but it also neglects correlations in

the evolution of the mean, effectively assuming that $\overline{\boldsymbol{f}(\boldsymbol{v}_{\mathrm{M}})} = \boldsymbol{f}(\bar{\boldsymbol{v}}_{\mathrm{M}})$; thus, this ad-hoc closure corresponds to imposing

$$
\begin{aligned}
a) & \quad \overline{\boldsymbol{v}'_{\mathrm{M}}\mathbf{B}^T(\boldsymbol{v}'_{\mathrm{M}},\boldsymbol{v}'_{\mathrm{M}}) + \mathbf{B}(\boldsymbol{v}'_{\mathrm{M}},\boldsymbol{v}'_{\mathrm{M}})\,\boldsymbol{v}'_{\mathrm{M}}{}^T} = 0, \\
b) & \quad \overline{\mathbf{B}(\boldsymbol{v}'_{\mathrm{M}},\boldsymbol{v}'_{\mathrm{M}})} = 0.
\end{aligned}
\tag{32}
$$

in (28). Note that the constraint (32b) is inconsistent with the nontrivial evolution of the covariance in (31b); see [4] for more details.

3.2.3   Mean Stochastic model (MSm)

The most simplified imperfect model we consider here uses the same moment closure approximations (32) as DMm but only accounts for the dynamics of the resolved variable $u(t)$ with the mean values of the unresolved variables in (24a), $\overline{\gamma} = \hat{\gamma}^M$ and $\overline{b} = 0$, resulting in the following linear, Gaussian model for the complex scalar u_{M}

$$
\dot{u}_{\mathrm{M}} = \left(-\hat{\gamma}^{\mathrm{M}} + i\omega^{\mathrm{M}}\right)u_{\mathrm{M}} + F^{\mathrm{M}}(t) + \sigma_u^{\mathrm{M}}\dot{W}_u(t).
\tag{33}
$$

The mean $\overline{u_{\mathrm{M}}}$ and covariance R_{M} for this linear model can be computed analytically in a standard fashion leading to the mean

$$
\bar{u}_{\mathrm{M}}(t) = e^{(-\hat{\gamma}^{\mathrm{M}}+i\omega^{\mathrm{M}})(t-t_0)}\bar{u}_0 + \int_{t_0}^t e^{(-\hat{\gamma}^{\mathrm{M}}+i\omega^M)(t-s)}F^{\mathrm{M}}(s)\mathrm{d}s,
\tag{34}
$$

and covariance $R_{\mathrm{M}} = \overline{\tilde{\boldsymbol{u}}'_{\mathrm{M}} \otimes \tilde{\boldsymbol{u}}'_{\mathrm{M}}{}^T}$ (considered in real variables $\tilde{\boldsymbol{u}}' = \left(\Re e[u'_{\mathrm{M}}], \Im m[u'_{\mathrm{M}}]\right)^T$ where $\tilde{\boldsymbol{u}}' = \tilde{\boldsymbol{u}} - \bar{\tilde{\boldsymbol{u}}}$)

$$
R_{\mathrm{M}}(t) = e^{\hat{A}(t-t_0)}R_0 e^{\hat{A}^T(t-t_0)} + \int e^{\hat{A}(t-s)}\hat{\Sigma}(s)e^{\hat{A}^T(t-s)}\mathrm{d}s, \qquad \hat{A} = \begin{bmatrix} -\gamma^{\mathrm{M}} & -\omega^{\mathrm{M}} \\ \omega_{\mathrm{M}} & -\gamma^{\mathrm{M}} \end{bmatrix},
\tag{35}
$$

with $\hat{\Sigma} = \frac{1}{2}\mathrm{diag}[(\sigma_u^{\mathrm{M}})^2, (\sigma_u^{\mathrm{M}})^2]$. Note that the linearity of the MSm implies that the covariance R_{M} is independent of the external forcing and, consequently, insensitive to forcing perturbations. Implications of this fact on improving the model fidelity and sensitivity are discussed in the following sections.

4   Uncertainty quantification and optimization of imperfect models for improved prediction skill

In this section we discuss uncertainty quantification and optimization of imperfect models for various prediction scenarios using the the stochastic-statistical framework and the suite of imperfect models introduced in the previous two sections. The considered scenarios are designed to elucidate the interplay between the climate fidelity of imperfect models and the initial conditions in short, medium and long range probabilistic predictions, as well as the sensitivity analysis to climate change scenarios where the system's attractor is perturbed. First, we focus on the probabilistic predictions in the perfect model setting where we point out the much longer memory of statistical initial conditions in non-Gaussian systems with intermittency compared to Gaussian systems; these long memory effects apply also to the initial conditions for the unresolved variables. The perfect system configuration is followed by a discussion of improvements in the predictive skill and sensitivity of imperfect models with significant model errors and overdamping after a simple optimization in the relative entropy metric by means of the stochastic noise inflation; the noise inflation is just one example of model improvement in this framework and other model parameters can be incorporated in more general approaches. Importantly, these results show usefulness of the principles advocated here in tough turbulent regimes with intermittency and energy transfer on the attractor.

The important points illustrated in the analysis and examples below are:

13

- Information-theoretic optimization of imperfect models can significantly improve model prediction skill and sensitivity to external perturbations (figures 4, 5). Statistical equilibrium/climate fidelity of imperfect models is necessary but not sufficient for high skill in forced response/climate change projections (figures 7-15).

- There exist barriers to improvements within a given class of imperfect models beyond which the loss of information in the imperfect models cannot be reduced (see, e.g., figure 6) except when the class of models is expanded to allow for more degrees of freedom.

- The sensitivity of imperfect models can be tested via FDT based on experiments in the training phase in the unperturbed statistical equilibrium/climate. Kicked response FDT seems very promising and it may be combined in the future with machine learning methods to devise kicked experiments.

- Nonlinear, non-Gaussian models can have long memory of initial conditions including the initial conditions for the unresolved processes (figures 2, 3). Linear Gaussian imperfect models cannot reproduce the response in the variance to forcing perturbations in climate change scenarios; the change in variability due to perturbations of the attractor of the true nonlinear system remain undetected by these models (see MSm in figures 7, 8, 10).

4.1   Perfect model predictions and the role of initial conditions

We study here the role of initial conditions in perfect model predictions over short, medium, and long time-periods. In particular, we illustrate the strong influence of the unresolved variables on the system memory. In order to mimic realistic situations, we construct a superensemble whose members consist of ensembles of initial conditions which are normally distributed around the climate mean with the climate variance at the initial time t_0; moreover, we assume that the initial conditions in each ensemble are known with high certainty, i.e., the variances associated with estimating the initial conditions are significantly smaller than the climate variance at t_0. In this statistical setup, two possibilities exist for making predictions of the future state of the system. One obvious strategy relies on Monte Carlo computations of path-wise predictions for each initial condition in every superensemble member, and subsequently collecting such predictions to determine the future statistical state of the system and the associated uncertainties. Here, instead of relying on the Monte Carlo estimates, we use the analytical formulas for the second-order statistics of the perfect model derived in [15], thus representing every superensemble member by its mean and covariance.

In figures 2-3 we show examples of such superensemble predictions together with the climate statistics for ensembles with different initial statistical conditions; in figure 2 the initial mean of the resolved variable $\langle u_0 \rangle$ is varied while the means of the hidden variables, $\langle b_0 \rangle$ and $\langle \gamma_0 \rangle$, are kept constant, while in figure 3 the resolved mean $\langle u_0 \rangle$ is constant and the initial mean of the hidden damping fluctuations $\langle \gamma_0 \rangle$ is varied. We consider predictions starting at two different times t_0 of the time-periodic cycle and we assume that the state of the system is known initially with a higher precision than given by the climate statistics, i.e. the variances of the superensemble members at t_0 are smaller than those given by the climate statistics at t_0. For clarity, the evolution of only two superensemble members with different initial means $\langle u_0 \rangle$ is shown for each initial time. The bottom panels in figures 2 and 3 show the gain of information beyond the climate statistics in the predictions with given initial conditions; the information gain is measured by the relative entropy $\mathcal{P}(\pi_{t_0}, \pi_{att})$, where $\pi_{t_0}(u, t)$ is the marginal density for the forecast with the initial condition at time t_0, and $\pi_{att}(u, t)$ is the time-periodic climate statistics. Unsurprisingly, the information gain of the forecasts approaches zero with increasing lead time; this fact is simply a consequence of the approach to the system's attractor and the loss of memory of the initial conditions. Since in our setup only the external forcing is time-dependent and the system parameters are constant, there is no significant difference in information when forecasting in different seasons.

In figure 3 we show forecasts for three different superensemble members with the same initial means for the resolved variable $\langle u_0 \rangle$ and different initial means of the hidden variable $\langle \gamma_0 \rangle$ representing the mean initial damping fluctuations of the resolved variable $u(t)$. Here, the gain of information beyond equilibrium and the memory of initial conditions is strongly affected by the initial mean state $\langle \gamma_0 \rangle$ of the 'unresolved' damping fluctuations; these memory effects become more pronounced with increasing deviation of the initial mean of damping fluctuations. Note that for the largest $\langle \gamma_0 \rangle$ most of the long range prediction skill resides in the variance which is reflected in the slow decay of the dispersion. This fact points to potentially important consequences of errors associated with treatment of unresolved damping fluctuations in imperfect models.

4.2   Climate fidelity, model error and information barriers

In any realistic climate science applications the evolution of a natural system is not known and, instead, imperfect models introducing various model errors must be used. Here, we consider the three imperfect models introduced in §3b to illustrate the impact of different model errors on the prediction skill over different lead times for the system (24) with intermittency and positive Lyapunov exponents. The two models based solely on the moment closure approximations, GCm and DMm, serve here to illustrate the effects of parameterization of unresolved scales; this setup can be regarded as an instructive example of model error due to neglecting turbulent fluxes from the unresolved scales which interact with the resolved scales in an intermittent fashion. Another common source of model error in prediction for high-dimensional systems arises when a subset of degrees of freedom of the perfect system is completely hidden from the family of its imperfect coarse-grained models. Here, we use MSm (§33.2), which only accounts for the resolved variable $u(t)$, to illustrate the effects this crude dimensional reduction on the prediction skill for the resolved component. The optimization procedure discussed in detail below for the imperfect models of §3 highlights the important issue of the existence of barriers to model improvement within a given class of imperfect models beyond which the loss of information in the imperfect models cannot be reduced except when the class of imperfect models is expanded to allow for more degrees of freedom.

4.2.1   Improving imperfect models through stochastic forcing

The moment closures employed in the derivation of GCm and DMm, or the dimensionality reduction used in MSm, do not guarantee a-priori the climate fidelity of these imperfect models. Important issues in this context concern (i) the effects of different moment closures on the climate statistics of the imperfect models, (ii) the extent of improvement in climate fidelity achieved by optimizing the model parameters through (6). Following the methodology of [38], we focus here on improving the model fidelity by inflating the stochastic forcing in the resolved dynamics of the imperfect models in order to minimize the annually averaged information content, $\overline{\mathcal{P}(\pi_{att}, \pi_{att}^{\mathrm{M}})}$, between the perfect and imperfect model climate. Note that while the noise inflation is sufficient for our purposes, larger sets of model parameters can be incorporated in more general approaches utilizing (6), depending on the model complexity and computational resources.

In figures 4-5 we show an example of such an optimization procedure carried out in regime II of mean-stable dynamics of the perfect system (24) and compare the statistics and the model error for the three imperfect models before and after optimal noise inflation. Clearly, for all imperfect models the climate fidelity is significantly improved by inflating the amplitude of the stochastic forcing $\sigma_u^{\mathrm{M}*}$. For GCm, the main improvement is in the dispersion part, since the signal error part for this model is very small throughout due to its correct treatment of the turbulent flux. For DMm the signal and dispersion contributions to model error are comparable before and after optimization with the post-optimization error significantly reduced. For MSm the model error in the unoptimized model is dominated by the dispersion part; after the noise inflation the signal and dispersion contributions to climate error are comparable and significantly reduced. We note here that for all models the total uncertainty in the climate was greatly reduced at all times although only the annually averaged climatology was used in the optimization procedure; this was observed earlier for the Gaussian models in [17].

Another important issue here concerns the extent to which the climate fidelity of the imperfect models of the system (24) can be improved in its different dynamical regimes with different characteristics of the transient instabilities. In the left column of figure 6 we show the optimal noise amplitude $(\sigma_u^{\mathrm{M*}})_{clim}$ for unperturbed climate fidelity and the corresponding annually averaged climate error as a function of the mean damping $\hat{\gamma}$ (top left) and as a function of the damping of fluctuations d_γ (bottom left). Recall that increasing $\hat{\gamma}$ decreases the decorrelation time of the resolved variable $u(t)$ and reduces the frequency of transient instabilities, leading to a transition between regimes II and III in the perfect dynamics of (24). For weak mean damping $\hat{\gamma}$, associated with very intermittent dynamics of $u(t)$ and fat-tailed marginal equilibrium PDFs, perfect climate fidelity cannot be achieved by inflating the stochastic forcing in the imperfect models. While the climate fidelity improves for all models for increasing $\hat{\gamma}$, GCm retains the best fidelity throughout. Analogous analysis for varying decorrelation time, $1/d_\gamma$, of the damping fluctuations γ such that $d_\gamma = \sigma_\gamma$ clearly shows existence of barriers to climate fidelity improvement by noise inflation as the hidden, transient instabilities become more abundant (see the transition between regimes II and I of (24) for increasing d_γ).

Finally, in in the right column of figure 6 we motivate and foreshadow the discussion of connections between climate fidelity and sensitivity of imperfect models to external forcing perturbations in a "climate change" scenario. It can be seen there that the optimized imperfect models, GCm and DMm, with good unperturbed climate fidelity also have a good skill for the climate change predictions, while MSm has a poor "climate change" prediction skill. A natural question here concerns the generality of such a relationship and possible tests which can be carried out in the unperturbed climate in order to probe the imperfect model sensitivity. The link (11) between the climate fidelity and sensitivity and its implications on long range prediction in systems intermittently positive Lyapunov exponents is examined in the following three sections.

4.3 Model sensitivity and climate change predictions for systems with intermittently positive Lyapunov exponents

The main focus of this section is on elucidating the link, discussed in §22.3 and illustrated in figure 6, between the climate fidelity of the imperfect models and their sensitivity to climate change scenarios induced by perturbations of the external forcing. Consequently, we consider here long lead times so that essentially all knowledge of the initial conditions is lost and only the perturbations to the statistical attractor of the perfect system due to forcing perturbations are important. More general situations involving the interplay between the memory of initial conditions and climate change, and imperfect model optimization for the short and medium range prediction skill are discussed in §34.4.

4.3.1 Perfect model response to the ramp-type forcing perturbations

Consider first the response of the perfect system (24) to deterministic perturbations of the external forcing $\delta F(t)$ which induce a change in the system attractor; this scenario will serve as a benchmark for the imperfect model considerations. In particular, we consider the following ramp-type perturbations of the time-periodic forcing (25)

$$\delta F(t) = (A_0^\delta - A_0)\frac{\tanh(a(t - t_c)) + \tanh(a\,t_c))}{1 + \tanh(a\,t_c))}, \tag{36}$$

with A_0^δ the perturbed mean forcing, A_0 the unperturbed mean forcing, and the parameter a controlling the time scale of the perturbation centered at time t_c. In order to mimic a climate change scenario, we assume that the system evolves initially on the unperturbed statistical attractor (climate) and subsequently, at time $t = 0$, the external forcing starts changing according to (36). The sensitivity of the perfect system to such perturbations of its attractor is quantified via the relative entropy $\mathcal{P}(\pi_{\delta F}, \pi_{att})$, as described in §22.1.

In the top left and bottom panels of figure 7 we show a typical example of perfect model sensitivity (black lines) in regime II (intermittent transient instabilities; figure 1) of the system (24); the top left panel shows the statistics of the resolved component $u(t)$ and the bottom panel shows the model sensitivity with corresponding signal and dispersion parts. The forcing perturbation (36) is applied with

$$A_0 = 4, \quad A_0^\delta = 4.4, \quad a = 0.3, \quad t_c = 20, \tag{37}$$

which corresponds to the change in the mean forcing by 10% over a period of about two years; the system evolution is monitored for another year after the forcing perturbation saturates. The nonlinearity of the perfect model is responsible for changes in both the mean and the variance in response to the forcing perturbations; it also induces changes in oscillation amplitudes induced by the perturbation. For this particular model with the typical mean forcing amplitudes chosen in (37) the signal part largely dominates the dispersion. For weaker mean forcing the effect of the dispersion on model error increases.

4.3.2 Perturbed climate predictions via imperfect models with optimal noise

We now turn to the issue of sensitivity of imperfect models with optimal noise to external forcing perturbations inducing a subsequent climate change.

Figure 7 illustrates these issues in a typical configuration in regime II (intermittent transient instabilities; figure 1) of the perfect model dynamics where both the perturbed statistics and perfect/imperfect model sensitivity are shown. The sensitivity of GCm and DMm is here comparable to the perfect model despite underestimating the response in the dispersion; as noted in the previous section this is a consequence of the signal dominated response of the perfect system (24). Clearly, disregarding completely the damping fluctuations in MSm leads to its failure in predicting the covariance response to the forcing perturbations; this is a direct result of the inherent linearization utilized in this model and occurs in all other dynamical regimes of the perfect system (24). This linearization has relatively little effect in regimes with no transient instabilities in the resolved dynamics (e.g., nearly-Gaussian regime III of (24); see figure 1), when the perfect system response in the mean is dominant; in such cases the sensitivity of all imperfect models in our suite is comparable with the perfect system (not shown). When abundant transient instabilities are present in the resolved dynamics $u(t)$, as in regime I (see figure 1) of (24), the perfect system sensitivity is dominated by the dispersion part which points to strong nonlinear effects. In such cases the sensitivity of all imperfect models is low compared to the perfect model (24) even with optimal stochastic forcing; this trend indicates an important role of the interaction between the third moments of the unresolved fluctuations, which are neglected in all the imperfect models examined here, and the resolved dynamics. Finally, we note that the sensitivity of GCm for the response in the mean remains very good in all dynamical regimes since, unlike the other two imperfect models, GCm retains the second moments of fluctuations in the evolution of the mean (30a).

4.3.3 FDT as a link between climate fidelity of imperfect models and their sensitivity

As already mentioned in §22.3 climate fidelity of an imperfect model does not guarantee its predictive skill and number of simple yet instructive examples can be found in [39]. The perfect system (24) considered here and its imperfect models GCm, DMm, and MSm are particularly interesting in this context since they provide nontrivial examples of climate change predictions in a system with intermittently positive Lyapunov exponents. Below, with the aim of elucidating the link discussed in §22.3, we study and compare climate change predictions based on the perfect system (24) with predictions obtained from the imperfect models with optimal stochastic forcing, and the corresponding predictions based on FDT. Recall that the link via FDT between climate fidelity of an imperfect model and its skill for predicting forced changes to the climate (unperturbed attractor) is directly linked to the skill in estimating the linear response operators for the mean and variance via (21) which can be evaluated in the training phase based on the measurements of the unperturbed climate.

17

The main points of this section are summarized in figures 8-11 where the response to forcing perturbations in the perfect and imperfect models with optimal noise is computed using both the kicked FDT and the quasi-Gaussian FDT (see §22.3) in two different dynamical configurations characteristic of regimes II and III (cf. §33.1 and figure 1). The forcing perturbation δF is the same in all cases and given by (36).

Figures 8-9 show an example of perfect/imperfect model predictions via FDT in regime III of (24), characterized by nearly Gaussian dynamics on the unperturbed attractor and strong damping of fluctuations in the resolved dynamics $u(t)$ (see figure 1); here $\hat{\gamma} = 8.2$ and approximately 16 moments are finite in the perfect marginal equilibrium PDF, the imperfect models are optimized for climate fidelity. The three columns in figure 8 show the true perturbed statistics predicted directly from the models (left), the statistics obtained using the kicked FDT (middle) and the statistics obtained from quasi-Gaussian FDT (right). Figure 9 shows the corresponding sensitivity (left) of the perfect system, $\mathcal{P}(\pi_{\delta F}, \pi_{att})$, and of the imperfect models $\mathcal{P}(\pi_{\delta F}^{\mathrm{M}}, \pi_{att}^{\mathrm{M}})$, the model errors of the kicked FDT (middle) for the perfect system $\mathcal{P}(\pi_{\delta F}, \pi_{\delta F}^{kck-FDT})$ and the models $\mathcal{P}(\pi_{\delta F}, \pi_{\delta F}^{\mathrm{M},\, kck-FDT})$, as well as the errors of qG-FDT (right), $\mathcal{P}(\pi_{\delta F}, \pi_{\delta F}^{qG-FDT})$, $\mathcal{P}(\pi_{\delta F}, \pi_{\delta F}^{\mathrm{M},\, qG-FDT})$ for the perfect system and the models respectively. In this regime the sensitivity of all models is comparable to the perfect model. Moreover, the skill of the kicked FDT is also very good in this regime for all three imperfect models; the differences between the imperfect models are insignificant compared to the perfect model sensitivity. For the quasi-Gaussian FDT, the errors in predictions utilizing GCm and DMm are comparable with the model sensitivity and have no skill; for the MSm the errors far exceed the model sensitivity.

The FDT predictions shown in figures 10-11 correspond to regime II of the system (24) characterized by a much weaker mean damping; here $\hat{\gamma} = 1.2$, in the resolved component $u(t)$ whose intermittent dynamics is associated with only few finite moments and fat algebraic tails in the equilibrium PDFs (two moments are finite for the parameters used). As before all models are optimized for the unperturbed climate fidelity. Clearly, the sensitivity of GCm and DMm remains here very good but MSm has a substantial error in the dispersion. This implies that completely neglecting the mean effects of the damping and forcing fluctuations on the resolved dynamics in MSm in the presence of intermittent bursts of instability at the resolved scales has the most detrimental effect on the prediction skill. Predictions based on kicked FDT retain high skill for GCm and moderately high skill for DMm. Neglecting the second moments of the unresolved fluctuations in the mean of DMm leads to a significant error in the FDT predictions which, however, remains small compared to the sensitivity of DMm. The kicked FDT predictions using MSm have a good skill for predicting the response in the mean in this regime but only a marginal overall skill due to significant errors in the dispersion. The predictions based on the quasi-Gaussian FDT have no skill in this regime, since the prediction errors far exceed the sensitivity for all models.

We note in summary that, similarly to the analysis carried out in [39] for a Gaussian turbulent tracer model (with no positive Lyapunov exponents), the kicked FDT emerges here as the best approach to make the forced response estimates in more realistic situations where direct predictions are impractical or impossible. Moreover, the kicked FDT based on GCm with optimal noise shows a good overall performance which is rivaled only by the perfect model predictions.

4.4 Predictive skill of imperfect models at short and medium ranges: Climate change and memory of initial conditions

We finally discuss the short and medium range predictive skill of the imperfect models when both the memory of the initial conditions and the climate change due forcing perturbations are important in the forecasts [5, 52, 20, 21].

In order to illustrate the effects of hidden instabilities on the predictive skill of different imperfect models with intermittently positive Lyapunov exponents, we consider two distinct dynamical configurations corresponding to (i) intermittent, large-amplitude bursts of transient instability in the resolved component $u(t)$ (regime II in §33.1 and in figure 1), and (ii) nearly Gaussian regime with essentially no transient instabilities in $u(t)$ (regime III in §33.1). As described in §22.1, the model error is quantified via the relative

entropy between marginal statistics of the perfect and imperfect models, $\mathcal{P}(\pi_{\delta F}(t|t_0), \pi_{\delta F}^{\mathrm{M}}(t|t_0))$, and the internal prediction skill is given by $\mathcal{P}(\pi_{\delta F}^{\mathrm{M}}(t|t_0), \pi_{att}^{\mathrm{M}}(t))$;

In figure 12 we show a typical example of imperfect model predictions in regime II of the mean stable dynamics of the system (24) for an ensemble of trajectories with statistical initial condition away from the unperturbed attractor; the system attractor is subsequently perturbed due to the changes in the forcing given by (36). The corresponding model error and internal prediction skill are shown in figure 13. Recall that in regime II of (see §33.1) the perfect system (24) the unresolved damping fluctuations affecting the resolved dynamics of u decorrelate much slower than in regime I; the resulting coarse-grained dynamics is characterized by intermittent, large-amplitude bursts of instability and fat-tailed equilibrium marginal PDF's. It is clear, by comparison of the total model error and the internal prediction skill, that GCm in this regime has a very good overall prediction skill including the short term evolution from given initial conditions and the long term perturbed climate consistency; the model error for GCm is dominated by the dispersion part which, however, is still smaller than the internal prediction skill for all times. Interestingly both, GCm and DMm also have short term prediction skill for the covariances alone and the dispersion part of their internal prediction skill is similar; however, GCm is much more skillful in this regime for predicting the mean. DMm has a good short range, and marginal long range prediction skill but it fails at the intermediate ranges during the forcing perturbation. MSm has no skill in this regime.

Figures 14-15 illustrate a typical situation of predictions in the nearly-Gaussian regime III of the perfect system (24) which is characterized by the lack of transient instabilities in the resolved dynamics $u(t)$. In this regime all imperfect models achieve perturbed climate consistency, as already discussed in §34.2. The model error for large lead times is dominated for all models by the signal part and it is significantly smaller than the long range internal prediction skill. GCm and DMm are essentially the same in this regime and have good prediction skill for all lead times. This indicates that the effects of neglecting the second moments in the mean and third moments in the covariance in the closure approximations has little effect in this regime. MSm, on the other hand, which completely neglects the dynamics of the unresolved variables for the (multiplicative) fluctuations in the damping and (additive) fluctuations in the forcing has no short range prediction skill as it fails to correctly account for the particular initial conditions; these effects transpire in both the signal and dispersion. Finally, we mention that in regime I of the perfect system (24), characterized by abundant short-lasting transient instabilities, GCm has a good skill for predicting the mean but it fails, like all the other imperfect models, at predicting the covariances which dominate the total model error.

5 Concluding remarks

Here, we discussed a range of important issues arising in applications of the newly emerging stochastic-statistical framework [37, 38, 39] to quantifying and mitigating uncertainties associated with prediction of partially observed and imperfectly modelled complex turbulent dynamical systems. This framework was tested on the statistically exactly solvable nonlinear and non-Gaussian 'perfect' system with hidden intermittent instabilities and large-scale, time-periodic features. The suite of imperfect models optimized to mimic the marginal statistics of the true resolved component on the attractor was used to illustrate various problems associated with dynamic prediction of complex turbulent dynamical systems. These include the role and mitigation of model error due to coarse-graining and dimensional reduction, moment closure approximations and the associated turbulent flux parameterization, and the memory of initial conditions in producing short, medium and long range forecasts and climate change scenarios (i.e., perturbations of the perfect system attractor). The mathematical tools employed here relied on empirical information theory and fluctuation-dissipation theorems and it was shown that they seamlessly combine into a concise systematic framework for measuring and optimizing consistency and sensitivity of imperfect models. Although this paper focused predominantly on the climate science applications, there are obvious analogues of the discussed techniques for uncertainty quantification and prediction in other areas dealing with complex dynamical systems with nontrivial high-dimensional attractors such as applications in neural

networks and materials science.

The following findings are particularly worth reiterating here:

- The information-theoretic optimization of imperfect models can dramatically improve the predictive performance and sensitivity of imperfect models to forced perturbations (see GCm in figures 7-15). However, the statistical attractor fidelity of imperfect models on the coarse-grained subset of resolved variables is necessary but not sufficient for high skill in climate change predictions (see DMm and especially MSm in figures 7-15).

- The information-theoretic optimization of imperfect models requires tuning of the marginal probability densities for the resolved variables with those of the perfect system on the unperturbed attractor (see (4) and figures 4, 5). In the simplest Gaussian framework such a procedure implies simultaneous tuning of means and covariances variances (see (9)) which is not substantially more expensive than the common tuning of the means.

- There exist barriers to improvements within a given class of imperfect models beyond which the loss of information cannot be reduced (see, e.g., figure 6). In such cases the class of imperfect models needs to be expanded in order to achieve further improvements.

- The sensitivity of imperfect models for capturing the effects of forced perturbations of the perfect system attractor can be tested via algorithms exploiting a suitable fluctuation dissipation theorem and experiments in the training phase in the unperturbed climate. Kicked response FDT seems very promising in this context (figures 9, 11) but additional work in this area is needed.

- Nonlinear, non-Gaussian models can have long memory of initial conditions, including the initial conditions for the unresolved processes (e.g., figures 2, 3). Linear Gaussian models cannot reproduce the forced response in the variance of the true nonlinear system. Consequently, the change in variability due to perturbations of the system's attractor remain undetected by linear imperfect models of a nonlinear system (see MSm in figures 7, 8, 10).

The results presented here and in [37, 38, 39, 17] further reinforce the utility of the information-theoretic framework for improving imperfect models through stochastic parameterization in climate change science or engineering applications. Clearly, much more work needs to be carried out in order to establish the usefulness of this approach in less idealized and much more complex cases such as the Global Circulation Models (GCMs). The illustrated link between climate fidelity and sensitivity obtained via the fluctuation-dissipation theorem opens up an enticing prospect of developing techniques for improving imperfect model sensitivity based on specific tests carried out in the unperturbed climate, especially since similar high skill for the kicked response FDT in the non-Gaussian tracer model has already been established in [39]. However, much more work in this area is needed in order to develop suitable techniques for detecting nature's kicks and monitoring their dissipation.

Acknowledgments

References

[1] R. V. Abramov, A. J. Majda, and R. Kleeman. Information theory and predictability for low-frequency variability. *J. Atmos. Sci.*, 62(1):65–87, 2005.

[2] H. Akaike. A new look at the statistical model identification. *IEEE Trans. Automatic Control*, 19:716–723, 1974.

[3] M.A. Alexander, L. Matrosova, C. Penland, J. D. Scott, and P. Chang. Forecasting Pacific SSTs: Linear Inverse Model Predictions of the PDO. *J. Climate*, 21:385–402, 2008.

[4] M. Branicki, B. Gershgorin, and A.J. Majda. Filtering skill for turbulent signals for a suite of nonlinear and linear kalman filters. *J. Comp. Phys*, 231:1462–1498, 2012.

[5] G. Branstator and H. Teng. Two limits of initial-value decadal predictability in a CGCM. *J. Climate*, 23(23):6292–6311, 2010.

[6] K. Burnham and D. Anderson. *Model selection and multimodel inference: A practical information-theoretic approach*. Springer Science, 2002.

[7] T. DelSole. Predictability and information theory. Part I: Measures of predictability. *J. Atmos. Sci.*, 61(20):2425–2440, 2004.

[8] T. DelSole. Stochastic model of quasigeostrophic turbulence. *Surveys in Geophysics*, 25(2):107–149, 2004.

[9] T. DelSole. Predictability and information theory. Part II: Imperfect models. *J. Atmos. Sci.*, 62(9):3368–3381, 2005.

[10] T. DelSole and J. Shukla. Model fidelity versus skill in seasonal forecasting. *J. Climate*, 23(18):4794–4806, 2010.

[11] K.A. Emanuel, J.C. Wyngaard, J.C. McWilliams, D.A. Randall, and Y.L. Yung. *Improving the scientific foundation for atmosphere-land ocean simulations*. Natl Acad Press, Washington DC, 2005.

[12] E.S. Epstein. Stochastic dynamic predictions. *Tellus*, 21:739–759, 1969.

[13] C. Gardiner. *Stochastic Methods: A Handbook for the Natural and Social Sciences*. Springer Series in Synergetics. Springer, Berlin, 4 edition, 2010.

[14] B. Gershgorin, J. Harlim, and A. J. Majda. Improving filtering and prediction of spatially extended turbulent systems with model errors through stochastic parameter estimation. *J. Comp. Phys*, 229(1):32–57, 2010.

[15] B. Gershgorin, J. Harlim, and A. J. Majda. Test models for improving filtering with model errors through stochastic parameter estimation. *J. Comp. Phys*, 229(1):1–31, 2010.

[16] B. Gershgorin and A. J. Majda. A test model for fluctuation–dissipation theorems with time-periodic statistics. *Physica D*, 239:1741–1757, 2010.

[17] B. Gershgorin and A. J. Majda. Quantifying uncertainty for climate change and long range forecasting scenarios with model errors. Part I: Gaussian models. *J. Climate*, 2012. accepted and in press.

[18] B Gershgorin and A.J. Majda. A nonlinear test model for filtering slow-fast systems. *Comm. Math. Sci.*, 6:611–649, 2008.

[19] B. Gershgorin and A.J. Majda. Filtering a nonlinear slow-fast system with strong fast forcing. *Comm. Math. Sci.*, 8:67–92, 2009.

[20] D. Giannakis and A. J. Majda. Quantifying the predictive skill in long-range forecasting. Part I: Coarse-grained predictions in a simple ocean model. *J. Climate*, 2011. accepted and in press, doi: 10.1175/2011JCLI4143.1.

[21] D. Giannakis and A. J. Majda. Quantifying the predictive skill in long-range forecasting. Part II: Model error in coarse-grained Markov models with application to ocean-circulation regimes. *J. Climate*, 2011. accepted and in press, doi: 10.1175/JCLI-D-11-00110.1.

[22] A. Gritsun and G. Branstator. Climate response using a three-dimensional operator based on the fluctuation-dissipation theorem. *J Atmos Sci*, 64:2558–2575, 2007.

[23] A. Gritsun, G. Branstator, and A.J. Majda. Climate response of linear and quadratic functionals using the fluctuation-dissipation theorem. *J Atmos Sci*, 65:2824–2841, 2008.

[24] M. Hairer and A.J. Majda. A simple framework to justify linear response theory. *Nonlinearity*, 12:909–922, 2010.

[25] A. H. Jazwinski. *Stochastic processes and filtering theory*. Academic Press, New York, 1970.

[26] L. Jia and T. DelSole. Diagnosis of Multi-year Predictability on Continental Scales. *J. Climate*, 24:5108–5124, 2011.

[27] R. Kleeman. Measuring dynamical prediction utility using relative entropy. *J. Atmos. Sci.*, 59(13):2057–2072, 2002.

[28] S. Kullback and R. Leibler. On information and sufficiency. *Ann. Math. Stat.*, 22:79–86, 1951.

[29] C.E. Leith. Climate response and fluctuation dissipation. *J. Atmospheric Sci.*, 32:2022–2025, 1975.

[30] E.N. Lorenz. Deterministic nonperiodic flow. *J. Atmos. Sci.*, 20:130–141, 1963.

[31] E.N. Lorenz. A study of predictability of a 28-variable atmospheric model. *Tellus*, 17:321–333, 1968.

[32] E.N. Lorenz. The predictability of a flow which possesses many scales of motion. *Tellus*, 21:289–307, 1969.

[33] A. J. Majda. *Real world turbulence and modern applied mathematics. In Mathematics: Frontiers and Perspectives 2000*, pages 137–151. International Mathematical Union, American Math. Society., 2000.

[34] A. J. Majda. Challenges in Climate Science and Contemporary Applied Mathematics. *Comm. Pure Appl. Math*, accepted and in press (2011).

[35] A. J. Majda, R. V. Abramov, and M. J. Grote. *Information Theory and Stochastics for Multiscale Nonlinear Systems*, volume 25 of *CRM Monograph Series*. Americal Mathematical Society, Providence, 2005.

[36] A. J. Majda and M. Branicki. Lessons in Uncertainty Quantification for Turbulent Dynamical Systems. *DCDS*, 2012. accepteed and in press.

[37] A. J. Majda and B. Gershgorin. Quantifying uncertainty in climage change science through empirical information theory. *Proc. Natl. Acad. Sci.*, 107(34):14958–14963, 2010.

[38] A. J. Majda and B. Gershgorin. Improving model fidelity and sensitivity for complex systems through empirical information theory. *Proc. Natl. Acad. Sci.*, 108:10044–10049, 2011.

[39] A. J. Majda and B. Gershgorin. Link between statistical equilibrium fidelity and forecasting skill for complex systems with model error. *Proc. Natl. Acad. Sci.*, 108, 2011.

[40] A. J. Majda, R. Kleeman, and D. Cai. A mathematical framework for predictability through relative entropy. *Methods Appl. Anal.*, 9(3):425–444, 2002.

[41] A. J. Majda and X. Wang. *Nonlinear Dynamics and Statistical Theories for Basic Geophysical Flows.* Cambridge University Press, Cambridge, 2006.

[42] A. J. Majda and X. Wang. Linear response theory for statistical ensembles in complex systems with time-periodic forcing. *Comm. Math. Sci.*, 8(1):145–172, 2010.

[43] A.J. Majda, R.V. Abramov, and M.J. Grote. *Information theory and stochastics for multiscale nonlinear systems.*, volume 25 of *CRM Monograph Series.* American Mathematical Society, Providence, Rhode Island, USA, 2005.

[44] A.J. Majda, J. Harlim, and B. Gershgorin. Mathematical strategies for filtering turbulent dynamical systems. *DCDS*, 27:441–486, 2010.

[45] J.D. Neelin, M. Munnich, H. Su, J.E. Meyerson, and C.E. Holloway. Tropical drying trends in global warming models and observations. *Proc Natl Acad Sci USA*, 103:6110–6115, 2006.

[46] B. K. Oksendal. *Stochastic Differential Equations: An Introduction with Applications.* Springer, 2010.

[47] T. Palmer. A nonlinear dynamical perspective on model error: a proposal for nonlocal stochastic dynamic parameterizations in weather and climate prediction models. *Quart J Roy Meteor Soc*, 127:279–303, 2001.

[48] C. Penland. *In Nonlinear Dynamics in Geosystems*, chapter Stochastic Linear Models of Nonlinear Geosystems. Springer, New York, 2007.

[49] C. Penland. *Climate Dynamics: Why does Climate Vary?*, chapter Chapter 4: A linear stochastic model of sea surface temperatures. Geophysical Monograph 189. The American Geophysical Union, 2010.

[50] C Penland and P. D. Sardeshmukh. The optimal growth of tropical sea surface temperature anomalies. *J. Climate*, 8:1999–2024, 1995.

[51] D. A. Randall. *Climate models and their evaluation. Climate change 2007: The physical science basis, contribution of working group I to the fourth assessment report of the intergovernmental panel on climate change*, pages 589–662. Cambridge University Press, 2007.

[52] H. Teng and G. Branstator. Initial-value predictability of prominent modes of North Pacific subsurface temperature in a CGCM. *Climate Dyn.*, 36:1813–1834, 2010.

[53] C. R. Winkler, M. Newman, and P. D. Sardeshmukh. A linear model of wintertime low-frequency variability. Part I: Formulation and forecast skill. *J. Climate*, 14:4474–4494, 2001.
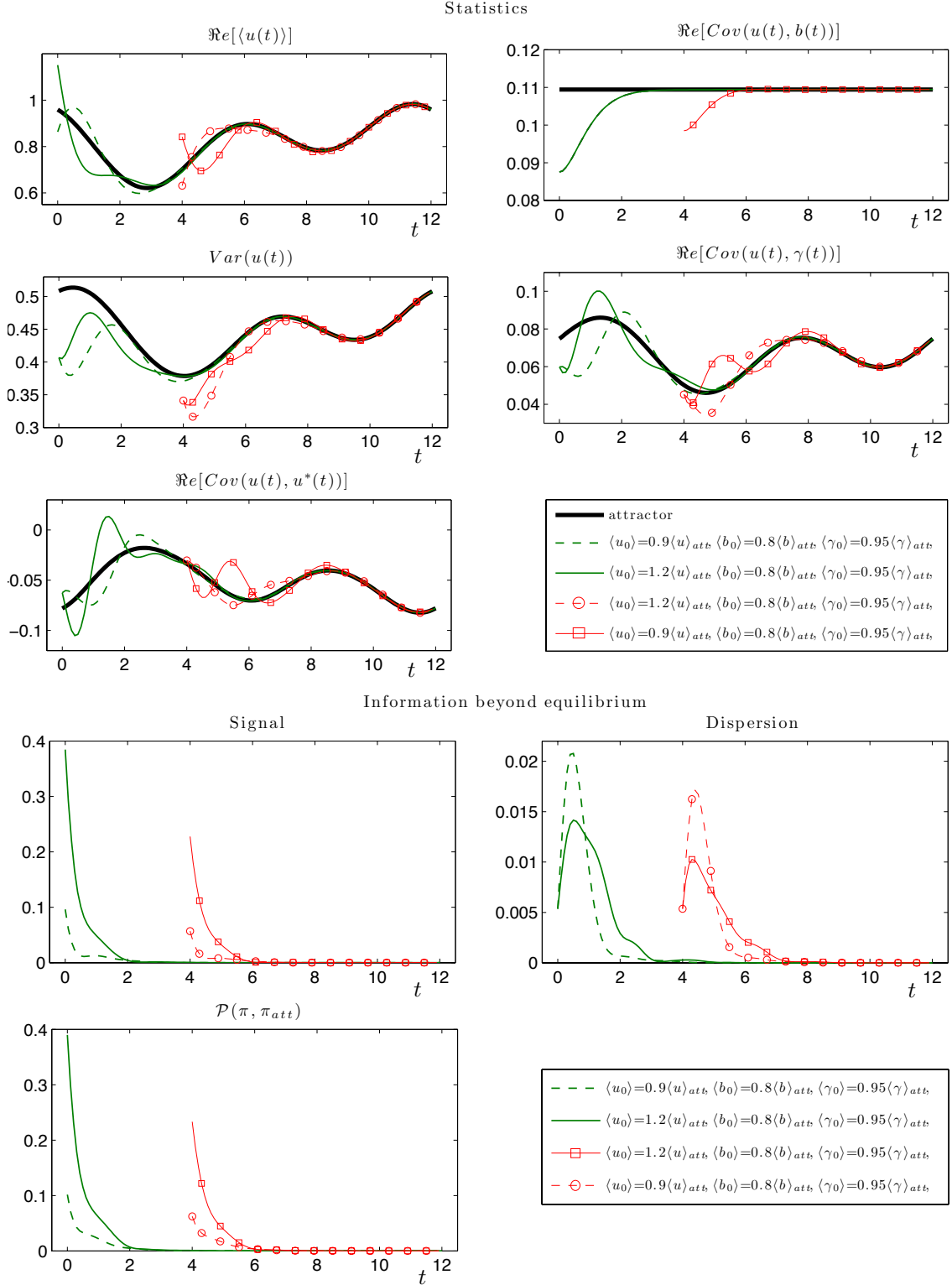
Figure 2: Perfect model forecasts (top panel) and associated information beyond equilibrium (bottom panel) with initial data sampled from the climate of the system (24). The thin lines (see legend) correspond to different ensembles of trajectories converging to the attractor (black) with the same initial means of the hidden variables, $\langle b_0 \rangle$ and $\langle \gamma_0 \rangle$, and different means of the resolved component $\langle u_0 \rangle$. Ensembles evolving from two different initial times are shown with $t_0 = 0$ (green) and $t_0 = 4$ (red); there is no significant difference in the information content for the forecasts starting at different phases of the cycle. This example corresponds to regime II (intermittent transient instabilities) of the perfect system (24) with forcing given by (25) and model parameters $\hat{\gamma} = 1.2, d_\gamma = \sigma_\gamma = 0.5$, $\sigma_u = 0.5$, (2 moments finite in equilibrium PDF).

Statistics

$\Re e[\langle u(t)\rangle]$

$\Re e[Cov(u(t), b(t))]$

$Var(u(t))$

$\Re e[Cov(u(t), \gamma(t))]$

$\Re e[Cov(u(t), u^*(t))]$

— attractor
— $\langle u_0\rangle=1.2\langle u\rangle_{att},\ \langle b_0\rangle=0.8\langle b\rangle_{att},\ \langle\gamma_0\rangle=0.8\langle\gamma\rangle_{att}$
- - $\langle u_0\rangle=1.2\langle u\rangle_{att},\ \langle b_0\rangle=0.8\langle b\rangle_{att},\ \langle\gamma_0\rangle=0.95\langle\gamma\rangle_{att}$
—◦— $\langle u_0\rangle=1.2\langle u\rangle_{att},\ \langle b_0\rangle=0.8\langle b\rangle_{att},\ \langle\gamma_0\rangle=1.2\langle\gamma\rangle_{att},$

Information beyond equilibrium

Signal

Dispersion

$\mathcal{P}(\pi, \pi_{att})$

— $\langle u_0\rangle=1.2\langle u\rangle_{att},\ \langle b_0\rangle=0.8\langle b\rangle_{att},\ \langle\gamma_0\rangle=0.8\langle\gamma\rangle_{att}$
- - $\langle u_0\rangle=1.2\langle u\rangle_{att},\ \langle b_0\rangle=0.8\langle b\rangle_{att},\ \langle\gamma_0\rangle=0.95\langle\gamma\rangle_{att}$
—◦— $\langle u_0\rangle=1.2\langle u\rangle_{att},\ \langle b_0\rangle=0.8\langle b\rangle_{att},\ \langle\gamma_0\rangle=1.2\langle\gamma\rangle_{att},$
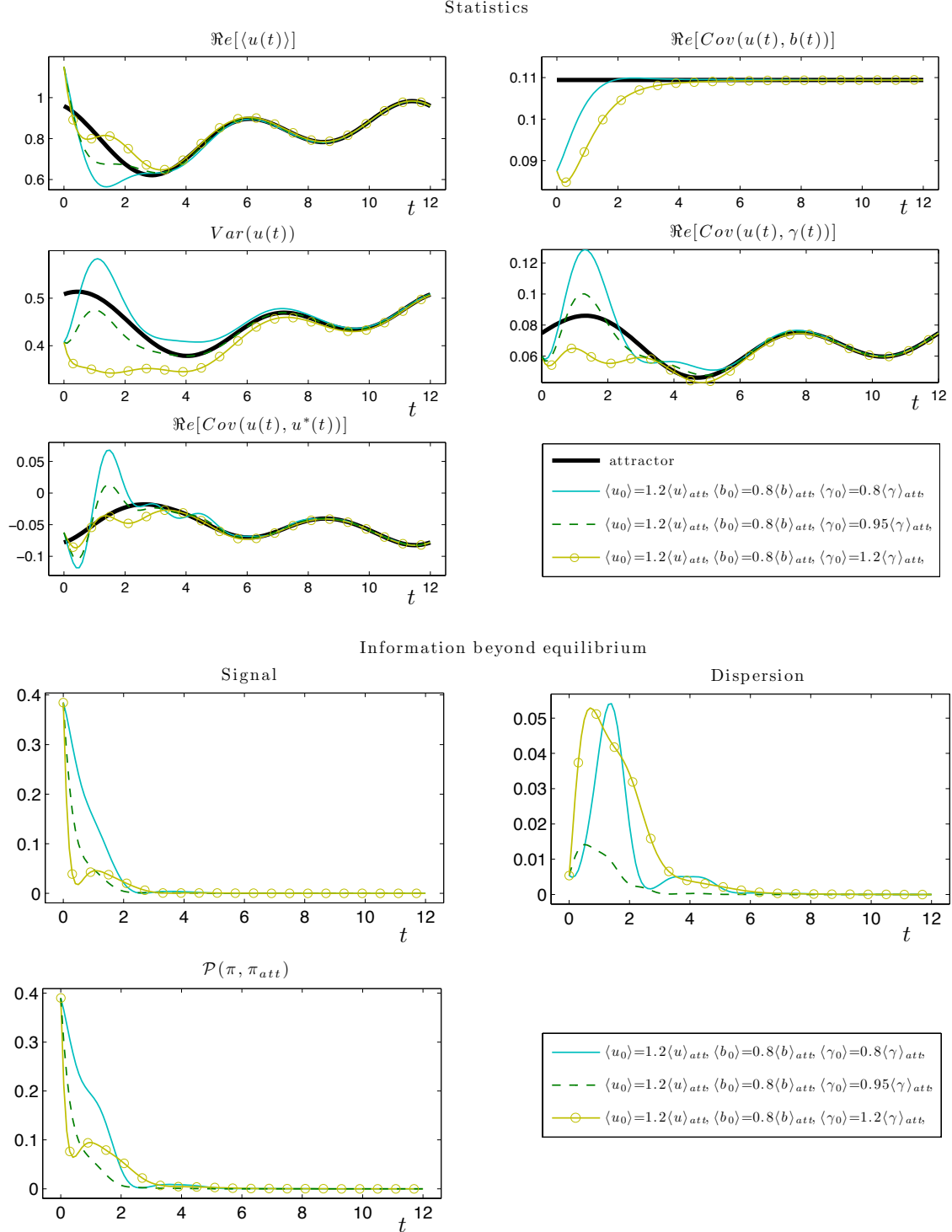
Figure 3: Effects due to the memory of initial conditions of hidden variables in perfect model forecasts (top) for the resolved component $u(t)$ in (24) and the associated information beyond equilibrium (bottom) with the initial data sampled from the climate/statistical equilibrium. The thin lines (see legend) correspond to different ensembles of trajectories converging onto the attractor (black) with the same initial means $\langle u_0\rangle$, $\langle b_0\rangle$ of the resolved component and the forcing fluctuations but different initial means of the damping fluctuations $\langle\gamma_0\rangle$. Note the significant differences in the information content beyond equilibrium for different hidden initial conditions $\langle\gamma_0\rangle$; the dispersion term of $\mathcal{P}(\pi_{t_0}, \pi_{att})$ dominates prediction skill $2 \lesssim t \lesssim 4$ when $\langle\gamma_0\rangle = 1.2\langle\gamma\rangle_{att}$. This example corresponds to regime II (intermittent transient instabilities) of the system (24) with the same parameters as in figure 2.
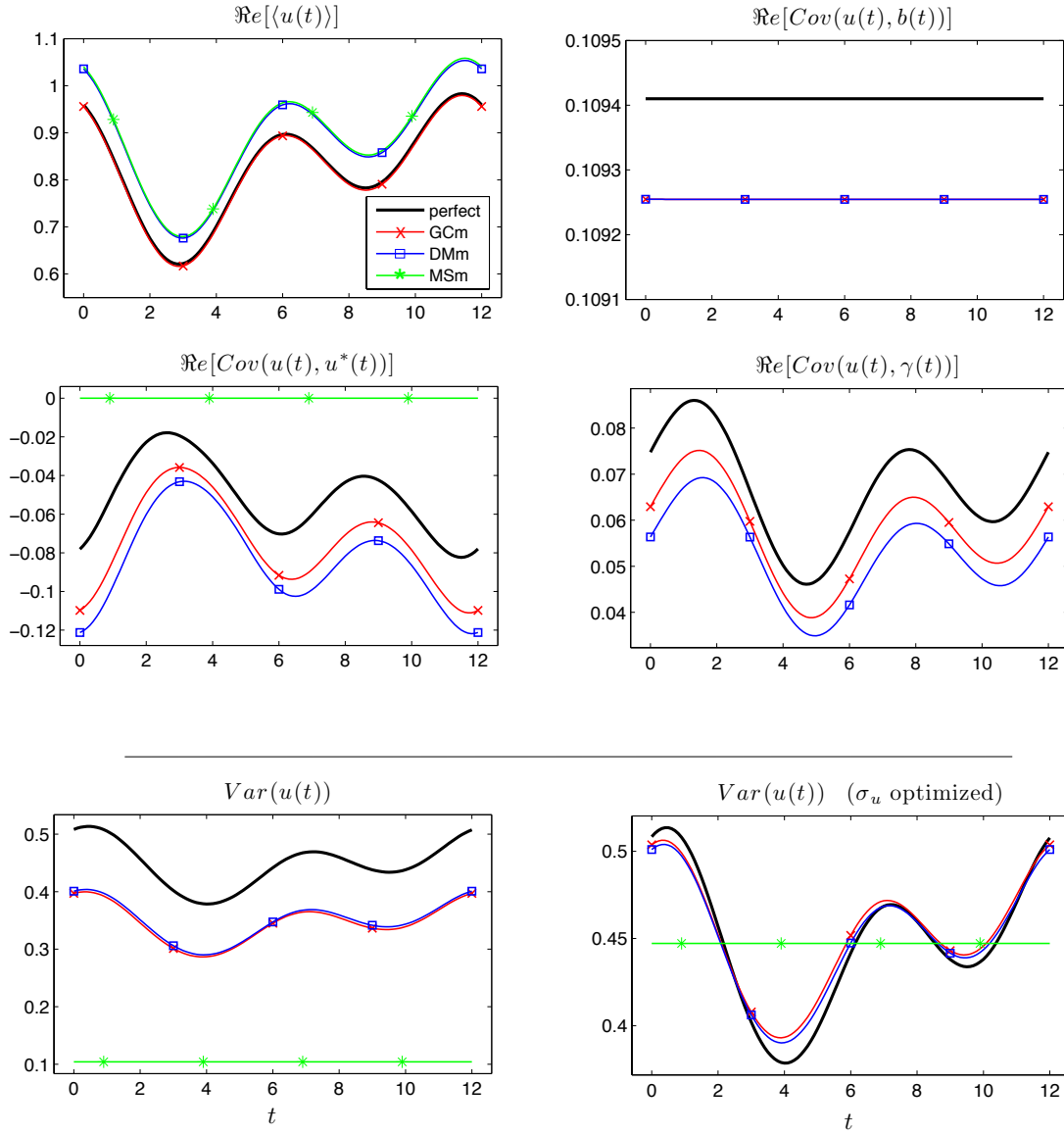
Figure 4: Equilibrium statistics associated with the resolved component $u(t)$ in the perfect and imperfect models for the complex scalar with hidden transient instabilities before and after optimal inflation of stochastic forcing. Note that only the variance is affected by the inflated noise. This example corresponds to regime II (intermittent transient instabilities with large amplitudes) of mean stable dynamics of the perfect system (24) with parameters $\hat{\gamma} = 1.2, d_\gamma = \sigma_\gamma = 0.5, \sigma_u = 0.5$, (2 moments finite in fat-tailed equilibrium PDF); the time-periodic forcing is given by (25).
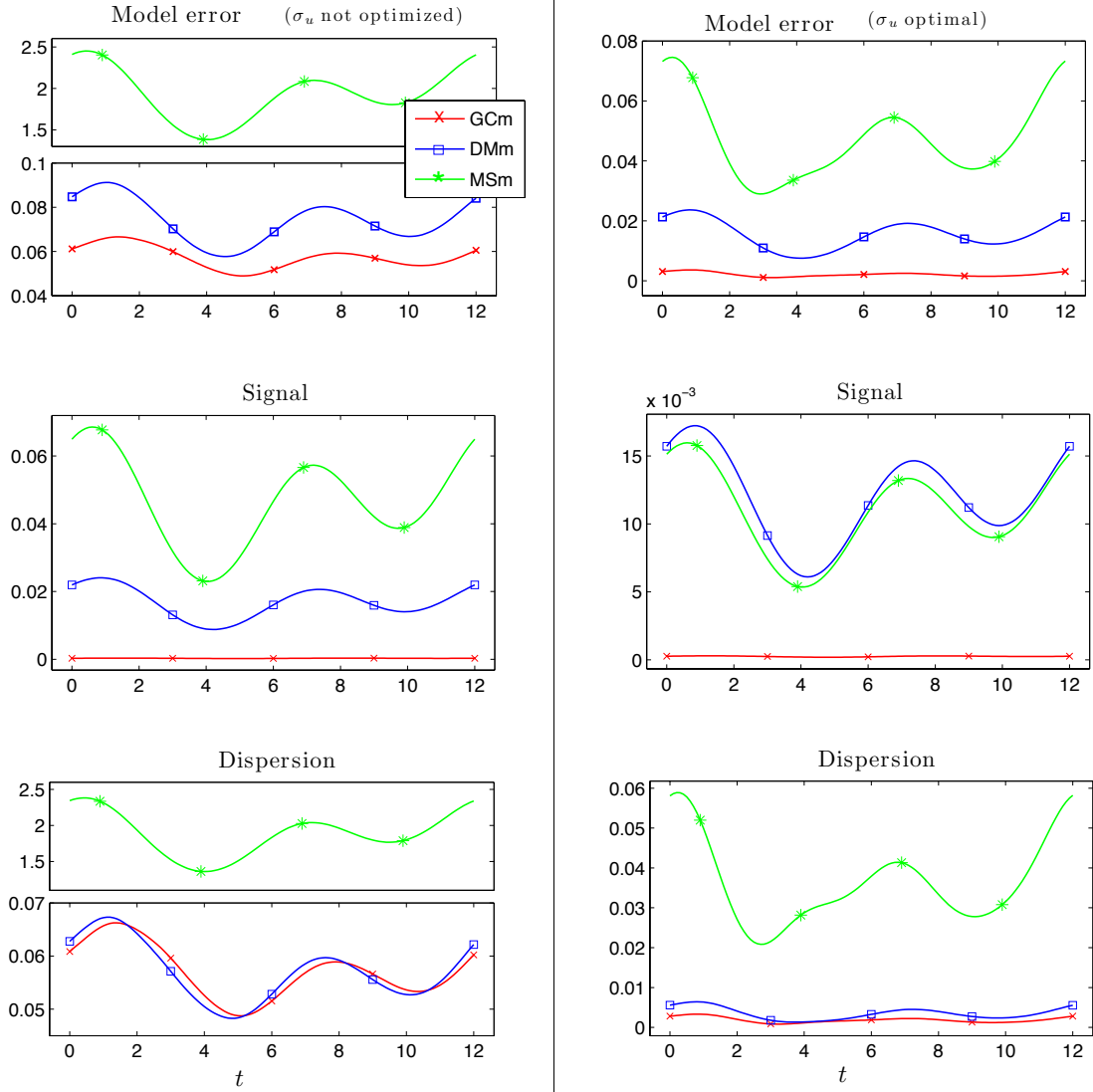
Figure 5: Model error in the climate expressed via the relative entropy, $\mathcal{P}(\pi_{att}, \pi_{att}^M)$, between the perfect and imperfect model statistics in the statistically steady state (see figure 4). The left column shows the relative entropy (top) and its signal (middle) and dispersion parts (bottom) for the original imperfect models. The right column shows analogous quantities for optimized imperfect models with inflated noise in the resolved component $u(t)$. Note the significant improvement, reflected in decrease of the relative entropy, in the optimized imperfect models compared to the original models without noise inflation.
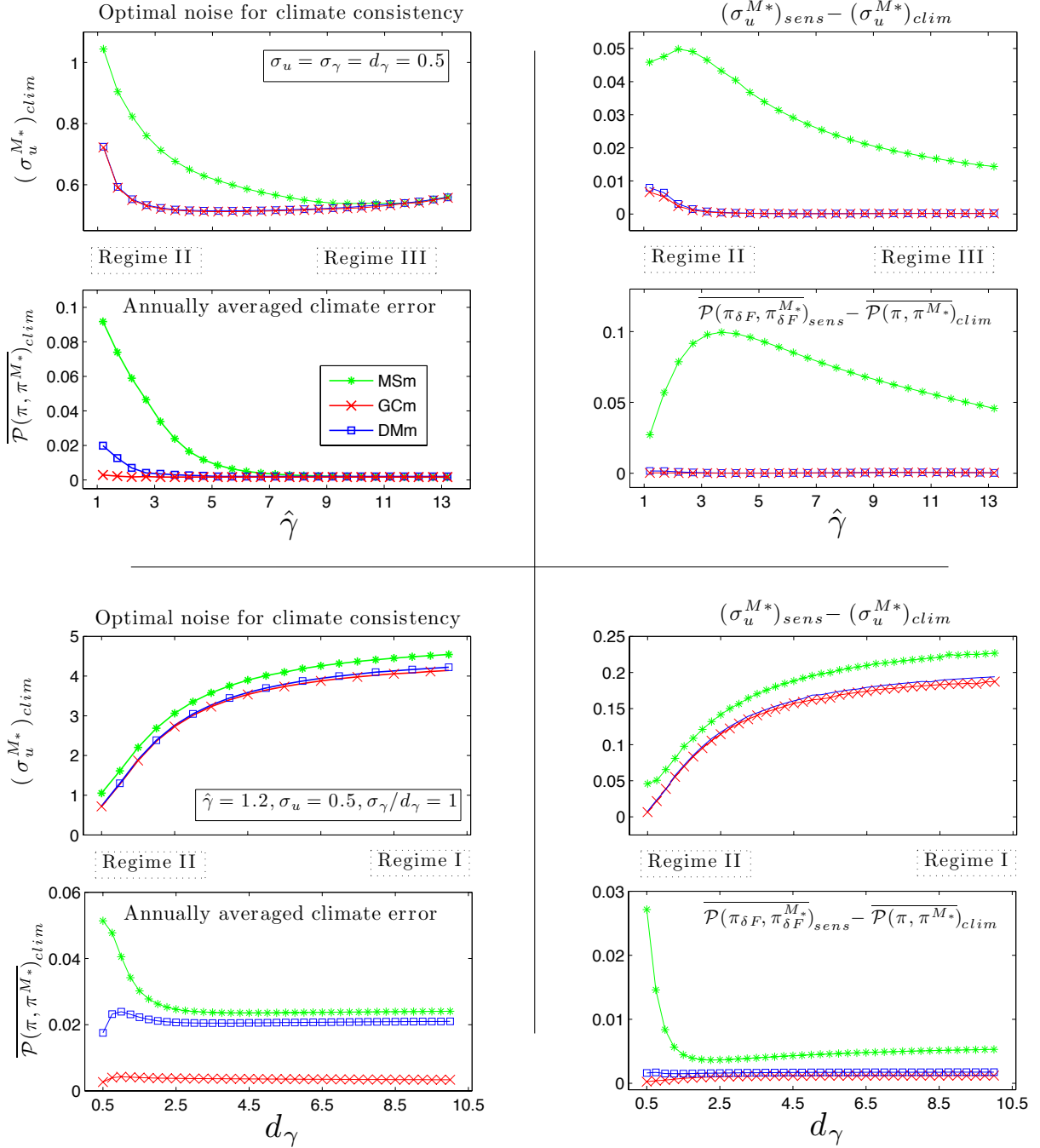
Figure 6: (Left column) Optimal noise amplitude $(\sigma_u^{M*})_{clim}$ for the unperturbed climate fidelity and the corresponding model error averaged over the annual cycle as functions of the mean damping $\hat{\gamma}$ (top left) and damping of fluctuations d_γ (bottom left) for the imperfect models GCm, DMm and MSm. The external forcing is given by (25) as in all previous examples. Note that for weak mean damping, $\hat{\gamma} \sim 1$, associated with very intermittent dynamics and fat-tailed marginal equilibrium PDFs for $u(t)$, perfect fidelity cannot be achieved by inflating the noise in the dynamics of $u(t)$. Note also the barrier to climate fidelity improvement by stochastic forcing inflation for increasing d_γ as the hidden, transient instabilities become more abundant in $u(t)$. (Right column) Illustration of the link (11) between climate fidelity and sensitivity showing differences between the noise amplitudes, $(\sigma_u^{M*})_{sens} - (\sigma_u^{M*})_{clim}$, and the error residuals, $\overline{\mathcal{P}(\pi_{\delta F}, \pi_{\delta F}^{M*})}_{sens} - \overline{\mathcal{P}(\pi, \pi^{M*})}_{sens}$, for imperfect models optimized, respectively, for the sensitivity to climate change and for the unperturbed climate fidelity. Note that the sensitivity optimization, which is practically unrealistic, can be achieved for GCm and DMm indirectly through optimization for unperturbed climate fidelity.
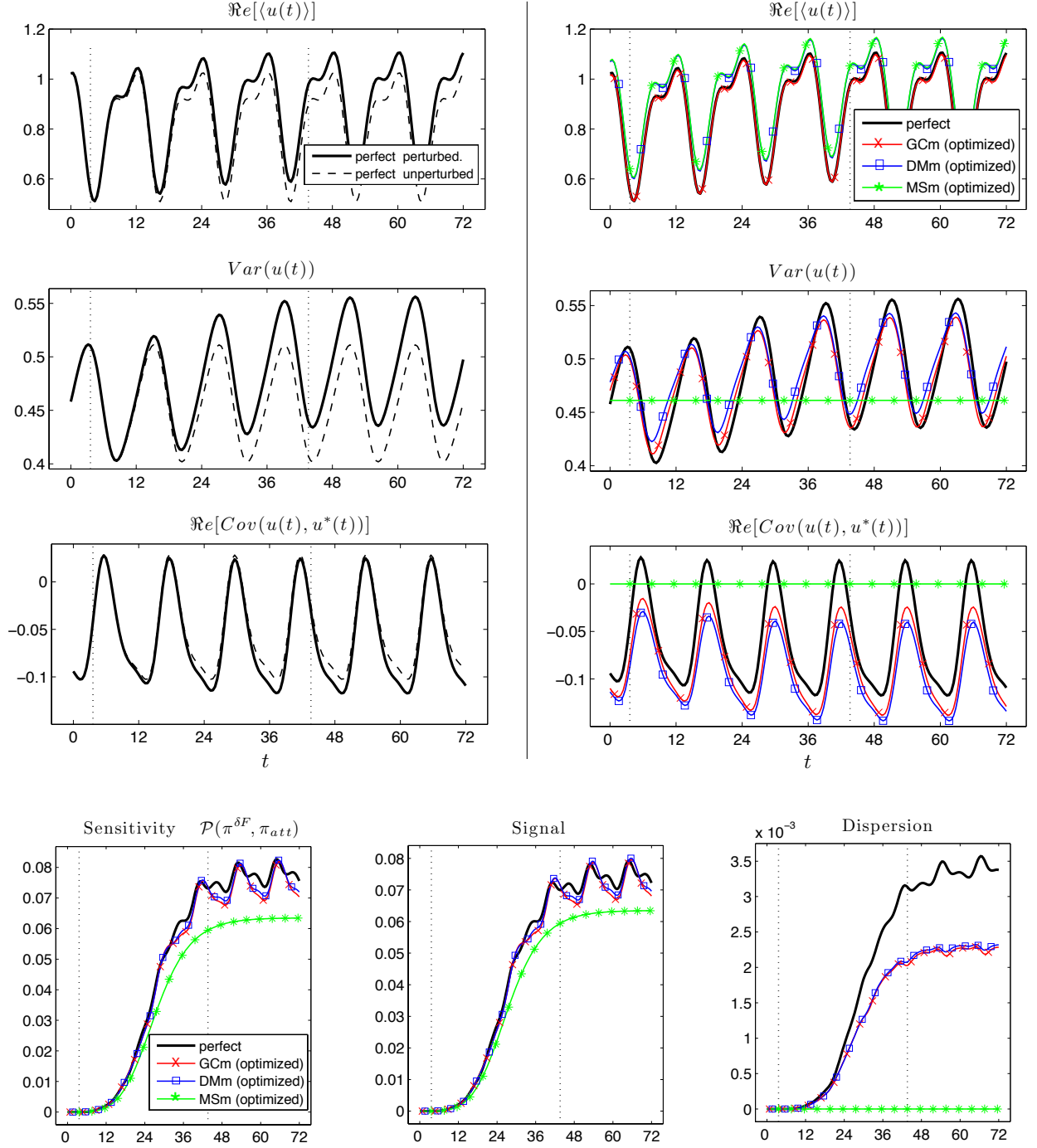
Figure 7: (Top left) Response of the statistics of the resolved component $u(t)$ in the perfect model (24) to ramp-type forcing perturbations δF given by (36) with parameters (37). (Top right) Analogous response computed from the imperfect models with optimal noise σ_u^{opt} in $u^M(t)$. (Bottom) The sensitivity of the perfect and imperfect models to the forcing perturbations expressed via the relative entropy, $\mathcal{P}(\pi_{\delta F}, \pi_{att})$, between the perturbed and unperturbed statistics. Note that MSm fails to reproduce the response in the covariance due to its inherent linearization. This example represents a typical situation in regime II of the perfect model dynamics (intermittent transient instabilities with large amplitudes in $u(t)$); in regime I (abundant transient instabilities) the perfect model response is dominated by the dispersion part and the sensitivity of all models deteriorates.

29
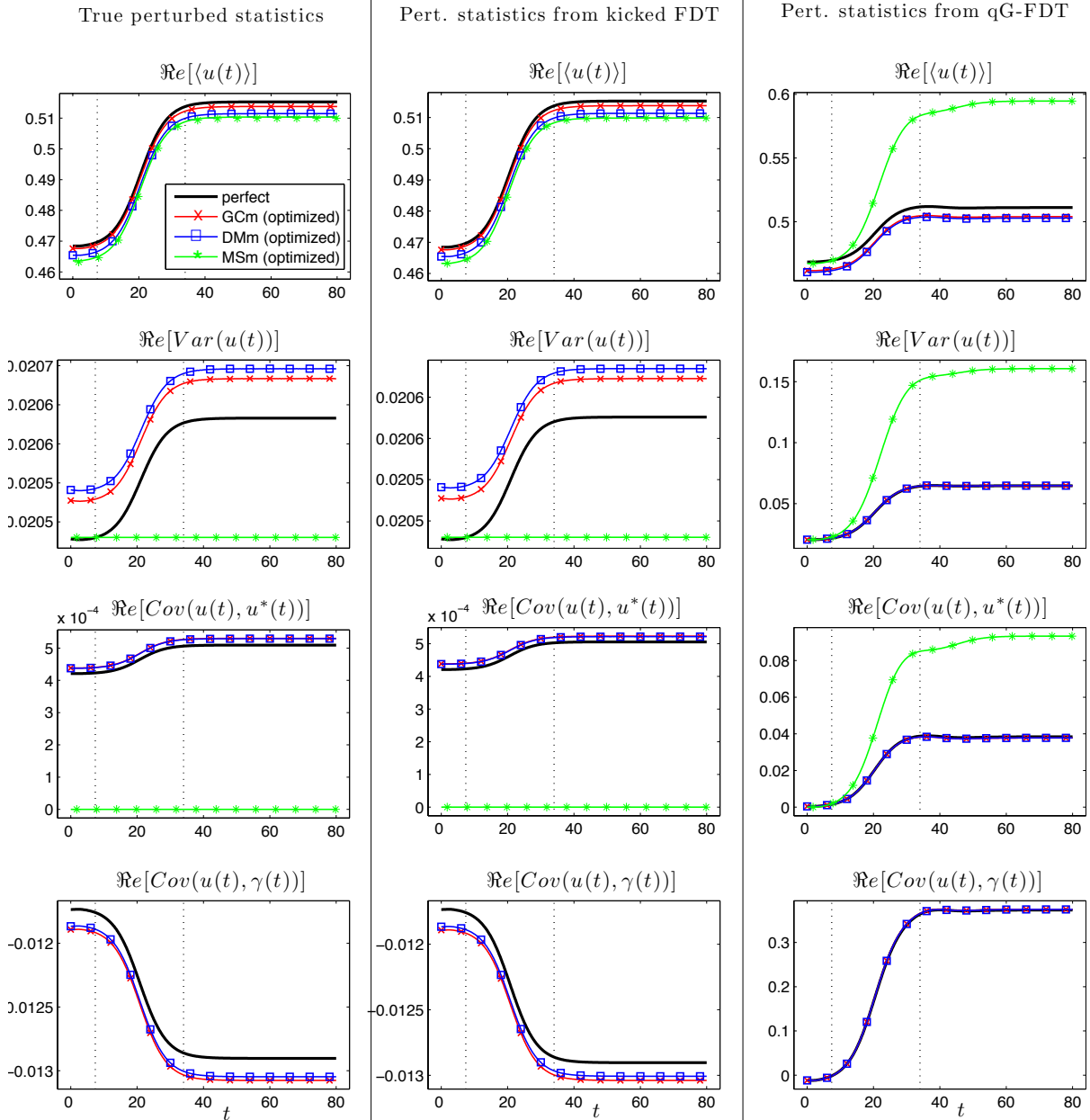
Figure 8: Example of perfect and imperfect model predictions in the (nearly-Gaussian) regime III of the system (24) for a climate change scenario associated with ramp-type perturbations δF (36) of constant external forcing; the corresponding model error and sensitivity are shown in figure 9. Left column shows the statistics of the resolved variable $u(t)$ predicted directly from the perfect system (thick black) and imperfect models (§33.2) with optimal noise for climate consistency. The middle and right columns show, respectively, the analogous predictions based on the kicked FDT and quasi-Gaussian FDT. The perturbation induces a 10% change in the forcing and the dashed vertical lines mark a region between 3% and 97% of the perturbation. The system parameters used here are $\hat{\gamma} = 8.2, d_\gamma = \sigma_\gamma = 0.5, \ \sigma_u = 0.5$ (16 moments finite in the marginal equilibrium PDF).
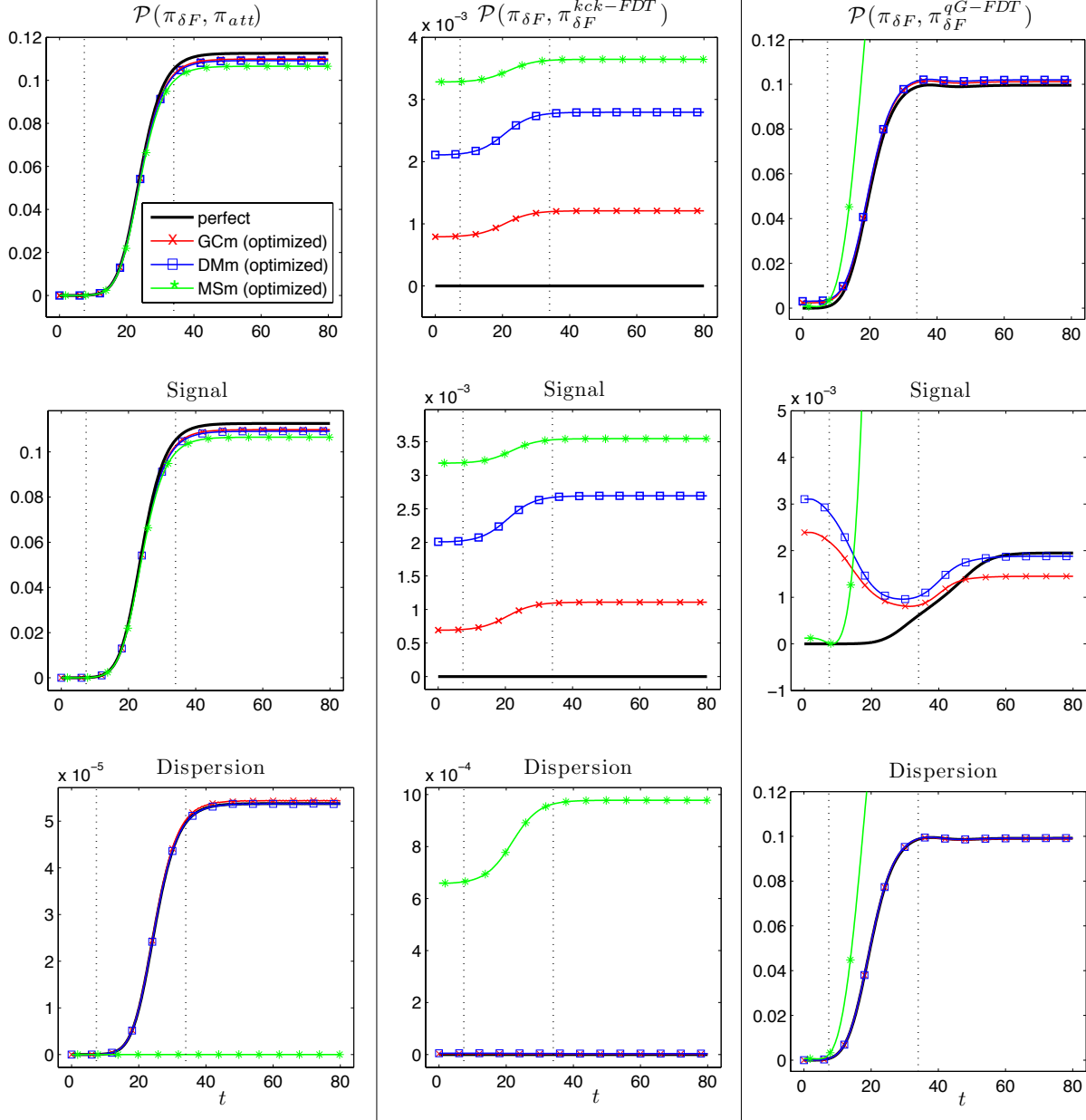
Figure 9: Sensitivity and model error via relative entropy for the perfect system and its imperfect models GCm, DMm, and MSm (see §33.2) corresponding to the climate change predictions shown in figure 8 in regime III of the perfect system (24). The left column shows the model sensitivity, and the middle and the right column show the error of climate change predictions using, respectively, kicked FDT and quasi-Gaussian FDT. Note that in this nearly-Gaussian regime the overall sensitivity of all imperfect models is comparable with that for the perfect system. However, the linear model, MSm, fails to reproduce the response in the covariances (see the Dispersion part of model sensitivity). The kicked FDT has overall good prediction skill for this climate change scenario for all models except for the Dispersion part of the error for the MSm; the Dispersion part of the error is here negligible compared to the Signal. The qG-FDT predictions (right column) have essentially no skill since the prediction errors for all models are, at best, comparable to the model sensitivity.
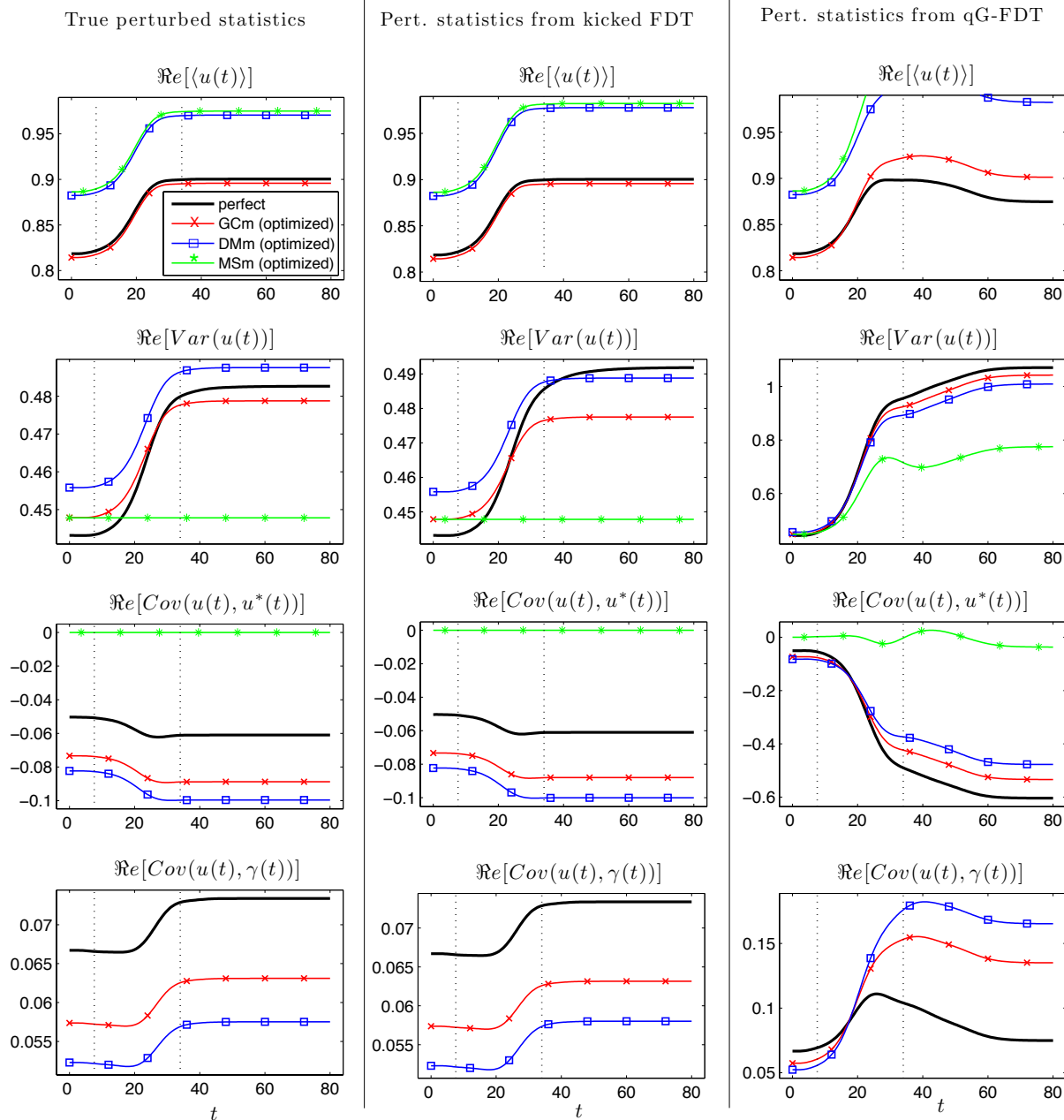
Figure 10: Example of perfect and imperfect model predictions in the regime II (intermittent, large-amplitude bursts of instability) of the system (24) for a climate change scenario associated with ramp-type perturbations δF (36) of constant external forcing; the corresponding model error and sensitivity are shown in figure 11. Left column shows the statistics of the resolved variable $u(t)$ predicted directly from the perfect system (thick black) and imperfect models (§33.2) with optimal noise for climate consistency. The middle and right columns show, respectively, the analogous predictions based on the kicked FDT and quasi-Gaussian FDT. The perturbation induces a 10% change in the forcing and the dashed vertical lines mark a region between 3% and 97% of the perturbation. The system parameters used here are $\hat{\gamma} = 1.2, d_\gamma = \sigma_\gamma = 0.5$, $\sigma_u = 0.5$ (2 moments finite in the marginal equilibrium PDF).
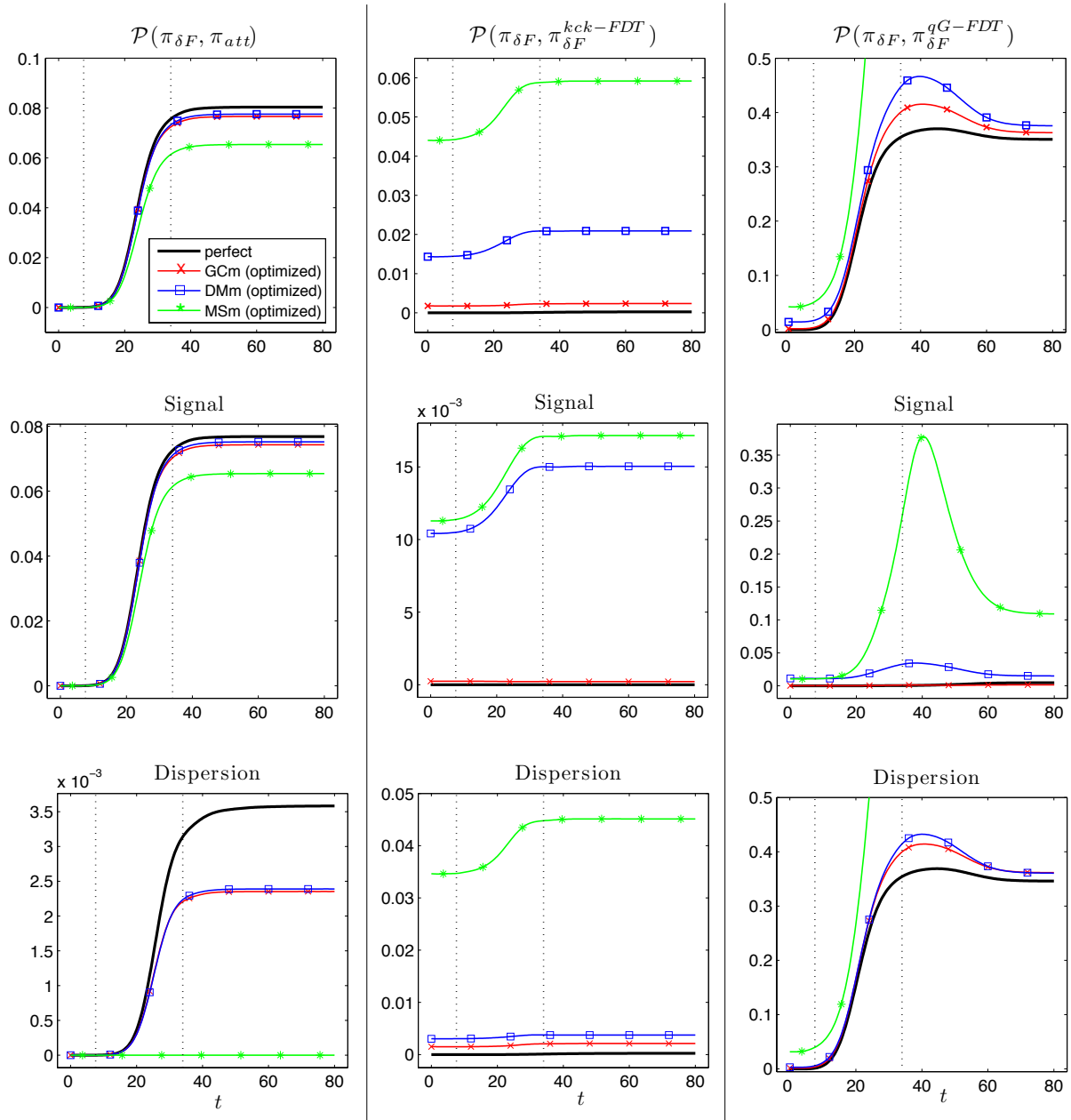
Figure 11: Sensitivity and model error via relative entropy for the perfect system and its imperfect models GCm, DMm, and MSm (see §33.2) corresponding to the climate change predictions shown in figure 10 in regime II of the perfect system (24). The left column shows the model sensitivity, and the middle and the right column show the error of climate change predictions using, respectively, kicked FDT and quasi-Gaussian FDT. Note that in this regime of intermittent transient instabilities the MSm, which completely neglects the damping fluctuations causing the instabilities, has a significantly lower sensitivity and large prediction errors, particularly in the Dispersion, for the climate change scenario studied. The kicked FDT has good prediction skill for GCm (very small errors for the mean response and acceptable errors for the covariance response) and moderate skill for DMm. The qG-FDT predictions (right column) have no skill since the prediction errors for all models far exceed the model sensitivity.
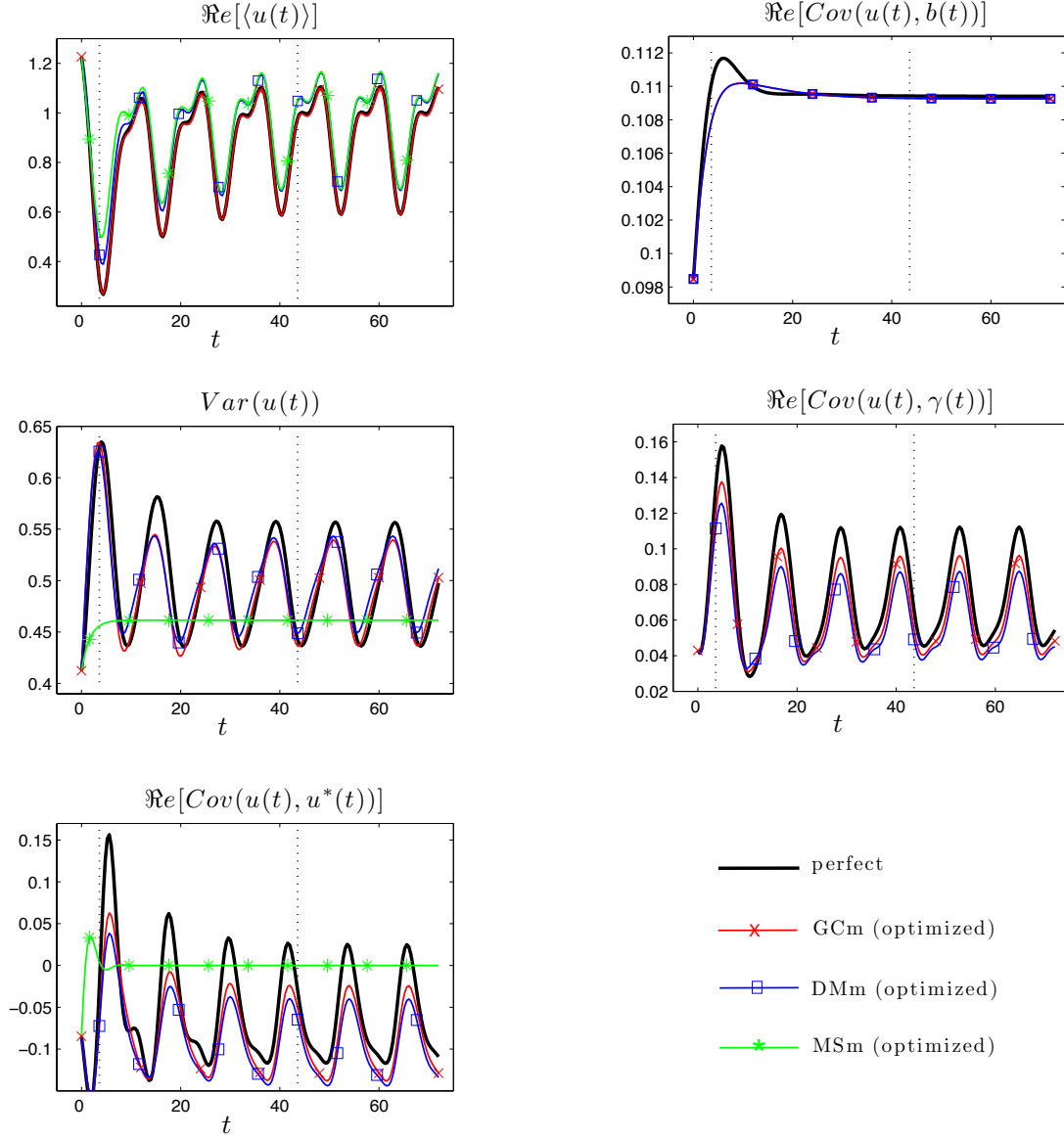
33

Figure 12: Example of perfect and imperfect model predictions with statistical initial conditions away from the attractor which is subsequently perturbed due to ramp-type changes in the external forcing; the unperturbed time-periodic forcing is given by (25) and the perturbations are represented by (36) with parameters (37). The dashed vertical lines mark a region between 3% and 97% of the perturbation. The corresponding model error and sensitivity are shown in figure 13. This example is typical of predictions in regime II (intermittent transient instabilities in the resolved component $u(t)$) of mean-stable dynamics of (24). The system parameters used here are $\hat{\gamma} = 1.2, d_\gamma = \sigma_\gamma = 0.5$, $\sigma_u = 0.5$ and the initial conditions are $\langle u_0 \rangle = 1.2 \langle u \rangle_{att}, \langle b_0 \rangle = 0.8 \langle b \rangle_{att}, \langle \gamma_0 \rangle = 0.8 \langle \gamma \rangle_{att}, R_0 = 0.85 R_{att}$.
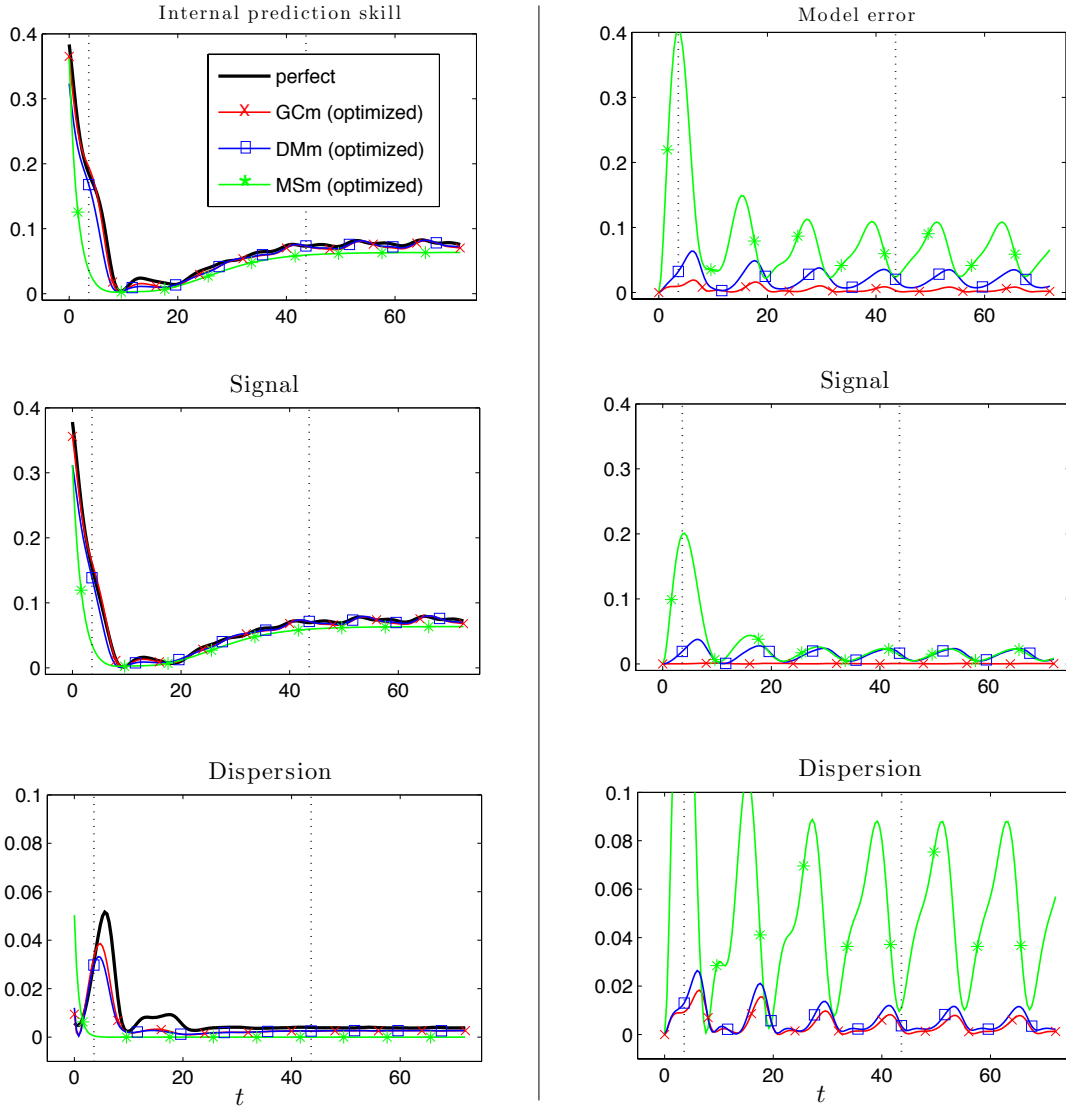
Figure 13: Model error via the relative entropy, $\mathcal{P}(\pi_{\delta F}(t|t_0), \pi_{\delta F}^M(t|t_0))$ (top panel), and the internal prediction skill, $\mathcal{P}(\pi_{\delta F}(t|t_0), \pi_{\delta F}^M(t|t_0))$ (bottom panel), for the predictions of the resolved component $u(t)$ shown in figure 12 for initial conditions at t_0 away from the attractor and a subsequent climate change due to forcing perturbations δF (36). Note the high skill of GCm at all ranges, including the short range skill in the dispersion. This situation is typical of regime II of the perfect model (24) where both GCm and DMm achieve perturbed climate consistency; MSm has no short range skill and only a marginal skill for the long range forecasts.
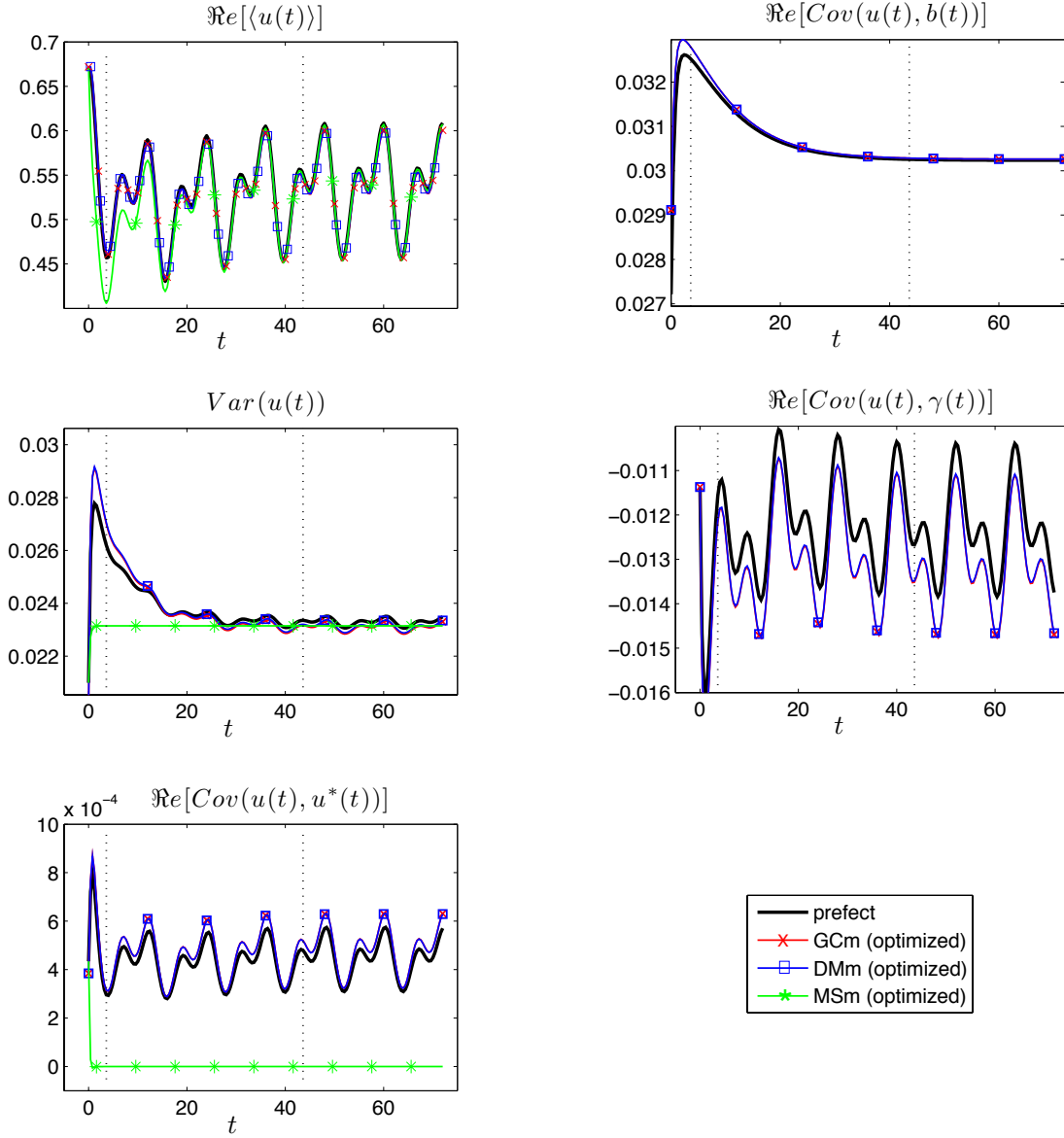
Figure 14: Example of perfect and imperfect model predictions with statistical initial conditions away from the attractor in the nearly-Gaussian regime III of the system (24). The attractor is subsequently perturbed due to ramp-type changes in the external forcing; the unperturbed time-periodic forcing is given by (25) and the perturbations, inducing a 10% change in the mean forcing, are represented by (36) with parameters (37). The dashed vertical lines mark a region between 3% and 97% of the perturbation. The corresponding model error and sensitivity are shown in figure 15. The system parameters used here are $\hat{\gamma} = 8.2, d_\gamma = \sigma_\gamma = 0.5$, $\sigma_u = 0.5$ and the initial conditions are $\langle u_0 \rangle = 1.2\langle u \rangle_{att}, \langle b_0 \rangle = 0.8\langle b \rangle_{att}, \langle \gamma_0 \rangle = 0.8\langle \gamma \rangle_{att}, R_0 = 0.85R_{att}$.
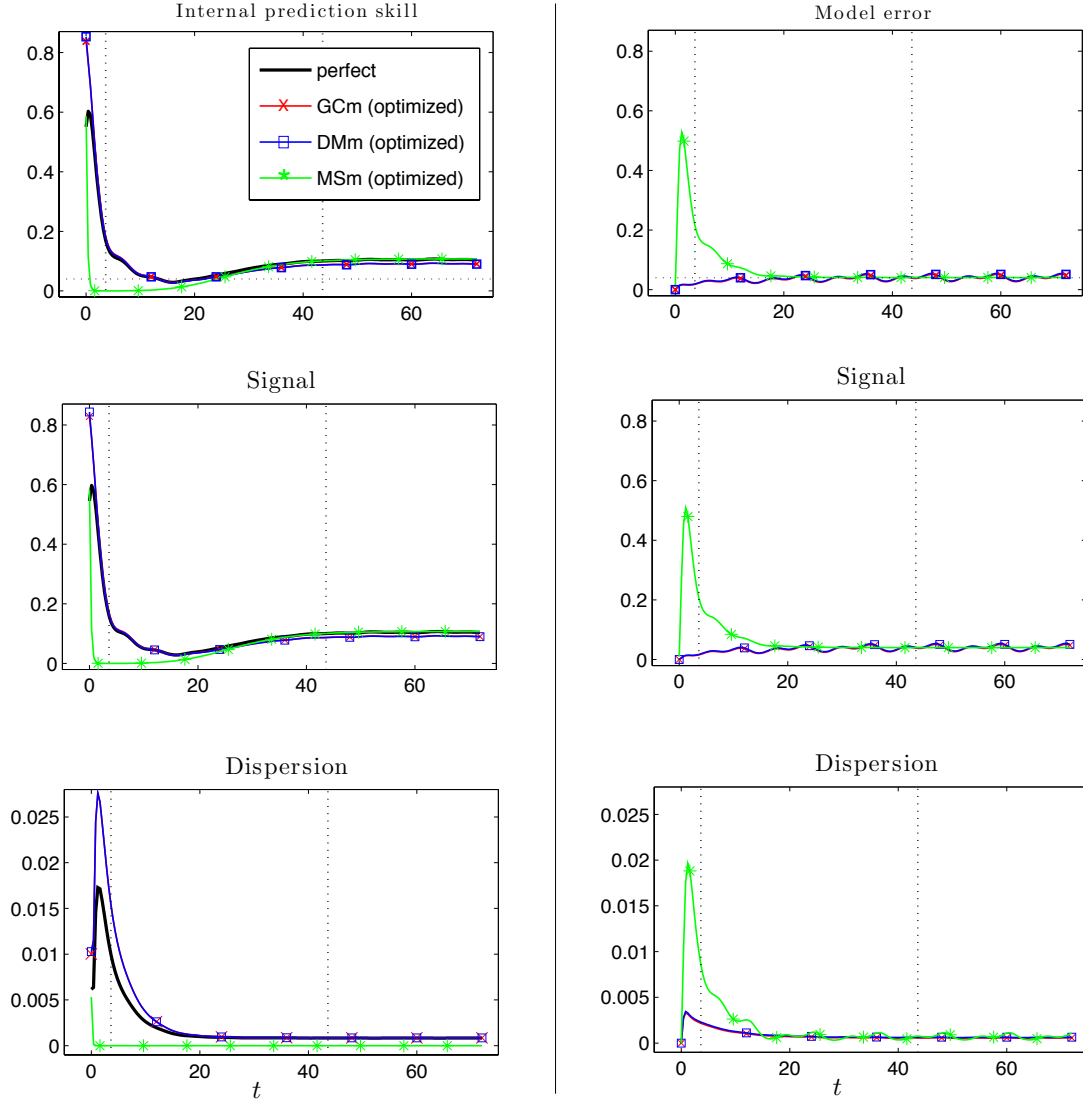
Figure 15: Model error via the relative entropy, $\mathcal{P}(\pi_{\delta F}(t|t_0), \pi_{\delta F}^M(t|t_0))$ (top panel), and the internal prediction skill, $\mathcal{P}(\pi_{\delta F}(t|t_0), \pi_{\delta F}^M(t|t_0))$ (bottom panel), for the predictions of the resolved component $u(t)$ shown in figure 14 for initial conditions at t_0 away from the attractor and a subsequent climate change due to forcing perturbations δF (36). Note the high skill of GCm and DMm at all ranges, including the short range skill in the dispersion. This situation is typical of the nearly Gaussian regime III of the perfect model (24) where all the imperfect models achieve perturbed climate consistency; MSm has no short range skill.

37